AD

NASA CR-54296
FA Report R-1796

FINAL REPORT

PLANE STRAIN FRACTURE TOUGHNESS AND MECHANICAL PROPERTIES OF 5Al-2.5Sn ELI TITANIUM AT ROOM AND CRYOGENIC TEMPERATURES

by

CARL M. CARMAN
JOHN W. FORNEY
JESSE M. KATLIN

Prepared for

NATIONAL AERONAUTICS AND SPACE ADMINISTRATION
Lewis Research Center

April 1966

NASA PURCHASE ORDER C6860A

UNITED STATES ARMY
FRANKFORD ARSENAL
PHILADELPHIA, PA.

NOTICE

This report was prepared as an account of Government sponsored work. Neither the United States, nor the National Aeronautics and Space Administration (NASA), nor any person acting on behalf of NASA

A.) Makes any warranty or representation, expressed or implied, with respect to the accuracy, completeness, or usefulness of the information contained in this report, or that the use of any information, apparatus, method, or process disclosed in this report may not infringe privately owned rights; or

B.) Assumes any liabilities with respect to the use of, or for damages resulting from the use of any information, apparatus, method or process disclosed in this report.

As used above, "person acting on behalf of NASA" includes any employee or contractor of NASA, or employee of such contractor, to the extent that such employee or contractor of NASA, or employee of such contractor prepares, disseminates, or provides access to, any information pursuant to his employment or contract with NASA, or his employment with such contractor.

DISPOSITION INSTRUCTIONS

Destroy this report when it is no longer needed. Do not return it to the originator.

The findings in this report are not to be construed as an official Department of the Army position unless so designated by other authorized documents.

NASA CR-54296
FA Report R-1796

FINAL REPORT

PLANE STRAIN FRACTURE TOUGHNESS AND MECHANICAL PROPERTIES OF 5Al-2.5Sn ELI TITANIUM AT ROOM AND CRYOGENIC TEMPERATURES

by

CARL M. CARMAN
JOHN W. FORNEY
JESSE M. KATLIN

prepared for

NATIONAL AERONAUTICS AND SPACE ADMINISTRATION
Lewis Research Center

April 1966

NASA Purchase Order C6860A

Technical Management
NASA Lewis Research Center
Chemical Rocket Division
Cleveland, Ohio
Richard N. Johnson and Gordon T. Smith

Pitman-Dunn Research Laboratories
FRANKFORD ARSENAL
Philadelphia, Pa. 19137

PLANE STRAIN FRACTURE TOUGHNESS AND MECHANICAL PROPERTIES OF 5Al-2.5Sn ELI TITANIUM AT ROOM AND CRYOGENIC TEMPERATURES

by

Carl M. Carman, John W. Forney, and Jesse M. Katlin

ABSTRACT

The suitability of 5Al-2.5Sn ELI titanium alloy for cryogenic tankage applications has been studied by determining the mechanical and fracture properties of the material at testing temperatures ranging from room temperature to -423° F. Small round tensile specimens were developed to measure the tensile properties over the range of testing temperatures. Plane strain fracture toughness measurements were also made at these temperatures using the "pop-in" technique with a small notched bend specimen.

Special laboratory techniques were developed to test the specimens at -423° F, utilizing the specific heat of vaporization of liquid helium.

The degree of preferred orientation in this alloy was qualitatively studied by determining the ratio of the width strain to the thickness strain. The fracture toughness values were interpreted in terms of the crystallography and mechanism of deformation of titanium.

The data are summarized in terms of a part-through defect which will be stable at various operating temperatures and stress levels. It has been shown that texture hardening may be used to obtain high burst stresses under biaxial stress conditions.

TABLE OF CONTENTS

List of Tables

List of Illustrations

Glossary

a - Notch depth or 1/2 crack length

A - Area

ß - Specimen thickness

d - Beam depth

D - Major diameter of notched round specimen

e - Engineering strain

E - Young's modulus

$\mathcal{E}$ - Energy

f' - $8.80 \times 10^{-5} \chi - 21.12 \times 10^{-5} \chi^2 + 76.08 \times 10^{-5} \chi^3$

$\mathcal{G}$ - Strain energy release rate

K - Parameter describing the local elevation of the elastic stress field ahead of a crack

K_{Ic} - Plane strain fracture toughness

ℓ - Beam span

ℓn - Natural logarithm

LD - Specimen longitudinal to rolling direct and crack propagating into the thickness direction of the plate

LS - Specimen longitudinal to rolling direction and crack propagation parallel to rolling plane

M - Bending moment

n - Strain hardening exponent

P - Load in pounds

Q - Form factor

r_{ys} - Radius of plastic strain zone

R - Ratio of width strain to thickness strain

T - Surface tension

TD - Specimen transverse to rolling direction and crack propagating into the thickness direction of the plate

TS - Specimen transverse to rolling direction and crack propagation parallel to rolling plane

W - Specimen width

α - (d - a)

β - Relative plastic zone size

ϵ - True strain

ν - Poisson's ratio

σ - Gross section stress

σ_{net} - Net section stress

σ_{nom} - Nominal stress

σ_{ys} - 0.2% offset yield stress

χ - a/d

ω - Work function

Subscripts

c - Critical value of a parameter

I - First, or opening, mode of fracture

PLANE STRAIN FRACTURE TOUGHNESS AND MECHANICAL PROPERTIES OF 5A1-2.5Sn ELI TITANIUM AT ROOM AND CRYOGENIC TEMPERATURES

by

Carl M. Carman, John W. Forney, and Jesse M. Katlin

Frankford Arsenal

SUMMARY

Inasmuch as future upper stage rockets will use liquid hydrogen as a fuel, the propellant tanks will be required to operate at -423° F. It is therefore desirable to employ materials for these structures which will possess very high strength-to-density ratios and material properties which will be satisfactory at the minimum operating temperatures. It appears that three types of alloys offer the promise of achieving the required high strength in combination with adequate fracture toughness at -423° F. This report presents engineering design data for one such material - an alpha titanium alloy.

The suitability of 5A1-2.5Sn ELI titanium alloy for cryogenic tankage applications has been studied by determining the mechanical and fracture properties of the material at testing temperatures ranging from room temperature to -423° F. Small round tensile specimens were developed to measure the tensile properties over the range of testing temperatures. Plane strain fracture toughness measurements were also made at these temperatures using the "pop-in" technique with a small notched bend specimen.

Special laboratory techniques were developed to test the specimens at -423° F, utilizing the specific heat of vaporization of liquid helium.

The degree of preferred orientation in this alloy was qualitatively studied by determining the ratio of the width strain to the thickness strain. The fracture toughness values were interpreted in terms of the crystallography and mechanism of deformation of titanium.

The data are summarized in terms of a part-through defect which will be stable at various operating temperatures and stress levels. It has been shown that texture hardening may be used to obtain high burst stresses under biaxial stress conditions.

INTRODUCTION

In the past, the majority of liquid-fueled rocket booster tanks have been constructed of either aluminum alloys or cold rolled stainless steel. The minimum operating temperature for these tanks has been that of the liquid oxygen contained in them, namely, -297° F. However, future upper stage rockets will use liquid hydrogen as a fuel and, therefore, the propellant tanks will operate at -423° F. It is doubtful if the presently used materials will operate efficiently at this temperature, due to either low strength or a deficiency in fracture toughness.

Because of the weight limitations in the upper stage structures of these new rockets, it would be desirable to employ materials possessing very high strength-to-density ratios, provided the material properties were satisfactory at the minimum operating temperatures. The aluminum alloys and cold rolled stainless steels used previously for rocket booster tanks have strength-to-density ratios of approximately 650,000 inches at room temperature and 850,000 inches at -297° F.

Data presented at the 1960 ASTM Symposium on Low Temperature Properties of High Strength Aircraft and Missile Alloys[1]* showed that these strength-to-density values can be exceeded substantially by some materials. Based on this published information, it appears that three types of alloys offer the promise of achieving high strength in combination with adequate fracture toughness at -423° F. These materials are: cold worked stable and metastable austenitic stainless steels, annealed alpha titanium alloys, and certain aluminum alloys of the copper-bearing series.

Since the alpha titanium alloys and the copper-bearing aluminum alloys offer the most promise in regard to high strength-to-density ratios, these materials were selected for investigation. This report presents engineering design data for an alpha titanium alloy. A subsequent report (NASA CR 54297) will be issued covering the aluminum work.

Program Objectives

The program objectives are:

(1) Provide basic design data for determining the maximum allowable flaw size for the onset of instability under plane strain conditions for 5Al-2.5Sn ELI titanium as a function of plate thickness and flaw orientation.

(2) Provide basic design data for the calculation of burst stress based on texture hardening of hexagonal close-packed metals.

*See REFERENCES

In view of the basic program objectives, this report is divided into two parts. The first part is concerned with the development of basic cryogenic design data and encompasses the fracture toughness and tensile testing at room and cryogenic temperatures; the second part deals with the texture-hardening properties of this material.

Materials

The material used throughout this investigation was 5Al-2.5Sn ELI (extra low interstitial) titanium alloy. The composition of this alloy is shown in Table I.

TABLE I
Composition of 5Al-2.5Sn ELI Titanium Alloy

Thickness (in.)	Percent							
	C	Fe	N	Al	H	Sn	Mn	O_2
1/2	0.023	0.16	0.010	5.0	0.001	2.6	0.006	0.086
1/4	0.023	0.16	0.010	5.0	0.000	2.6	0.006	0.080

The material was received as 1/4 and 1/2 inch thick hot rolled plates. These plates were annealed by furnace cooling from 1500° F.

BASIC DESIGN DATA - FRACTURE TOUGHNESS

The first objective of this program can be achieved by the application of Griffith-Irwin fracture mechanics. This concept is based on the early work of Griffith[2] using an ideally brittle material - glass. Mr. Griffith postulated that, at instability, the strain energy released per unit crack extension was equal to twice the surface tension per unit crack extension, as shown in Equation 1.

$$\frac{d\,\mathcal{E}_c}{B\ da} \geq \frac{2T}{B\ da} \qquad (1)$$

The relationship expressed in Equation 1 has been experimentally verified for glass. However, attempts to apply this simple relationship to more ductile materials, such as metals, resulted in discrepancies of several orders of magnitude. This was attributed to the work absorbed by plastic deformation at the crack tip, which is not considered in this equation.

Later, Irwin[3] proposed that a work function be substituted for the surface tension term. Therefore, Equation 1 becomes, at instability,

$$\frac{d\mathcal{E}_c}{B\ da} \geq \frac{d\omega}{B\ da} \tag{2}$$

where ω = work function, which is composed of two terms: surface tension and plastic deformation.

Inglis[4] developed the stress analysis for a through crack in an infinite plate, so that Equation 2 becomes

$$\frac{d\omega}{dA} = \mathcal{G} = \frac{\pi\ \sigma^2 a}{E} \tag{3}$$

Recently, Irwin[5] has proposed that the events at the leading edge of a crack be described in terms of a parameter, K, which is a function of the local elevation of the elastic stress field ahead of the crack. It may be shown that

$$E\ \mathcal{G} = K^2 \qquad \text{(plane stress)} \tag{4}$$

and

$$\frac{E\ \mathcal{G}_I}{(1-\nu^2)} = K_I{}^2 \quad \text{(plane strain)} \tag{5}$$

In the definition of the problem, we are primarily concerned with the first (subscript I) or opening mode of fracture. This situation is illustrated in Figure 1. Under these conditions, the displacements are in the y direction only, and the plastic deformation is confined to a small area adjacent to the crack tip.

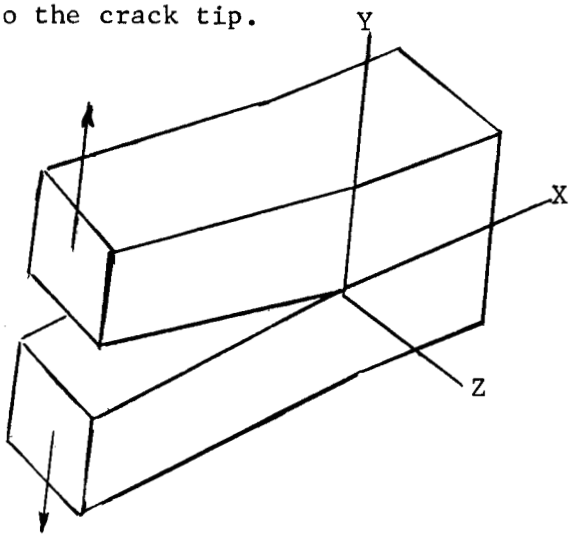

Figure 1. First, or opening, Mode of Fracture

Approach

Plane strain conditions require maximum elastic constraint in the path of crack extension. Specimen geometries must be designed with this requirement in mind.

Historically, the circumferentially notched-fatigue cracked round has been the most popular specimen and for this specimen, the plane strain fracture toughness, K_{Ic}, may be calculated from

$$K_{Ic} = \frac{0.233\ \sigma_{net}\ (\pi D)^{1/2}}{\left(1 - \frac{K_{Ic}^2}{2\sigma_{ys}^2\ \pi D}\right)^{1/2}} \tag{6}$$

The major difficulty with such a specimen is the need for large specimen diameters, so that $\sigma_{net} \leq 1.1\sigma_{ys}$ to avoid general yielding of the net section.

Irwin[6] has developed a stress analysis to measure the stress intensity, K_I, for a part-through semi-elliptical crack. His expression is given as

$$K_I = 1.1\ \sigma \left(\frac{\pi a}{Q}\right)^{1/2} \tag{7}$$

For valid K_{Ic} measurements utilizing this analysis, the gross section stress must not exceed the yield strength nor the crack depth exceed one-half the plate thickness. Quite frequently, these requirements necessitate the use of large and costly specimens.

Recently Boyle, Sullivan, and Krafft[7] described a technique for measuring the plane strain fracture toughness using sharply notched sheet specimens. This technique is based on the fact that the initial burst of crack growth from the starting notch or fatigue crack is under plane strain conditions. The load at "pop-in" is usually detected by an inflection in the load-deflection curve of the specimen. The plane strain fracture toughness is calculated from the load at "pop-in" using the initial crack length and the appropriate plane stress equation. For a center crack sheet, this would be

$$K_{Ic} = \sqrt{\sigma^2 W \tan\left(\frac{\pi a}{W} + \frac{K^2}{2W\sigma_{ys}^2}\right)} \tag{8}$$

The development of the "pop-in" technique for measuring the plane strain fracture toughness has resulted in a further decrease in specimen size, as evidenced by the recent use of the single-edge notched specimen. The plane strain fracture toughness is calculated from a compliance calibration of the specimen or from an analytical relationship recently developed by Gross.[8]

It is also possible to measure the plane strain fracture toughness in slow notched bending. The plane strain fracture toughness for three-point loading may be calculated from a compliance calibration developed by Irwin[9], and is given as

$$K_{Ic} = \sqrt{\frac{1}{d}\left(\frac{P}{B}\right)^2 \frac{(\ell/d)^2}{12.7 \times 10^{-6}} \quad (f')} \qquad (9)$$

where $f' = 8.80 \times 10^{-5}\ \chi - 21.12 \times 10^{-5}\ \chi^2 + 76.08 \times 10^{-5}\ \chi^3$.

An analytical solution has also been derived by Bueckner[10] to calculate K_I in notched bending. His expression for K_I per unit thickness is given as

$$K_I = \frac{6M}{(d-a)^{3/2}} f\left(\frac{a}{d}\right) \qquad (10)$$

The values of f(a/d) are given in Table II.

TABLE II
Value of f(a/d) as a Function of a/d

a/d	0.05	0.10	0.20	0.30	0.40	0.50	0.60
f(a/d)	0.36	0.49	0.60	0.66	0.69	0.72	0.73

Luban[11] has shown that both the compliance calibration and Bueckner's solution give almost identical results. In addition, Kies et al[12] have stipulated that, for valid K_{Ic} measurements in slow notch bending, the nominal fiber stress at the root of the notch should not exceed 1.1 σ_{ys} and that the most appropriate notch depth is 0.2 to 0.3 of the beam depth.

Specimen Selection

The requirement to measure the plane strain fracture toughness at -423° F necessitates the use of a small specimen. Employing larger specimens of the circumferentially notched round or part-through crack variety would require excessive amounts of cryogenic coolants. Therefore, a small slow-notched bend specimen was selected to best fit these requirements. By employing the "pop-in" method, the physical size of the specimen could be further reduced. The specimen which was selected for the cryogenic studies is shown in Figure 2. The thickness and depth of the notched beam specimen can be varied within the limits of the mechanical test equipment without altering the accuracy of the plane strain fracture toughness analysis.

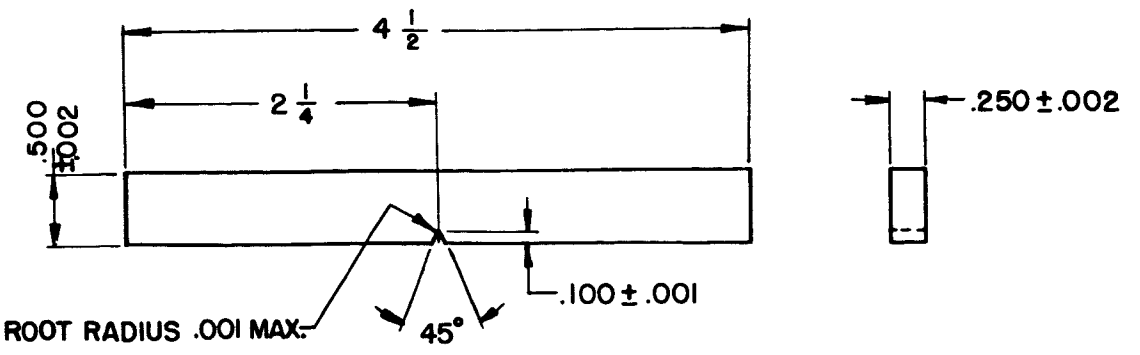

Figure 2. Small Notched Bend Specimen

Unpublished work at Frankford Arsenal has shown that the load at "pop-in" may be readily detected by a small high-elongation strain gage placed at the crack tip. With the advent of suitable techniques for attaching and using strain gages at these low temperatures, this method of "pop-in" detection should give reliable data without incorporating an additional large mass requiring greater cooling capacity.

As mentioned previously, large consumptions of cryogenic coolants and the mechanical limitations of the cryostat necessitated the use of small specimens for K_{Ic} determinations. This also held true for the determination of the engineering tensile properties. Therefore, a small round tensile specimen (0.160 in. diameter), as shown in Figure 3, was used for these studies. Small strain gages were used to determine the strain of the specimen.

To provide supporting fracture toughness data for the notched bend specimens, a small single-edge notched specimen was used. A drawing of this specimen is shown in Figure 4.

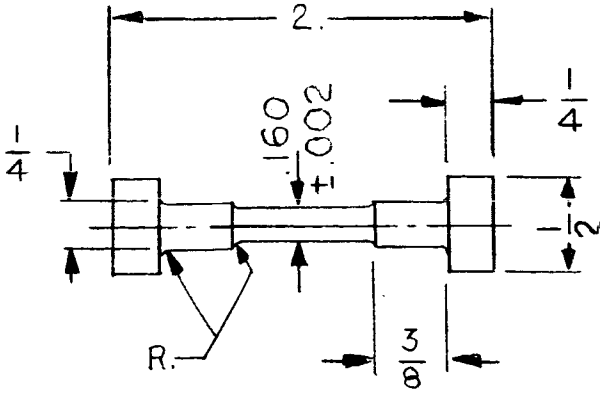

Figure 3. Small round Tensile Specimen

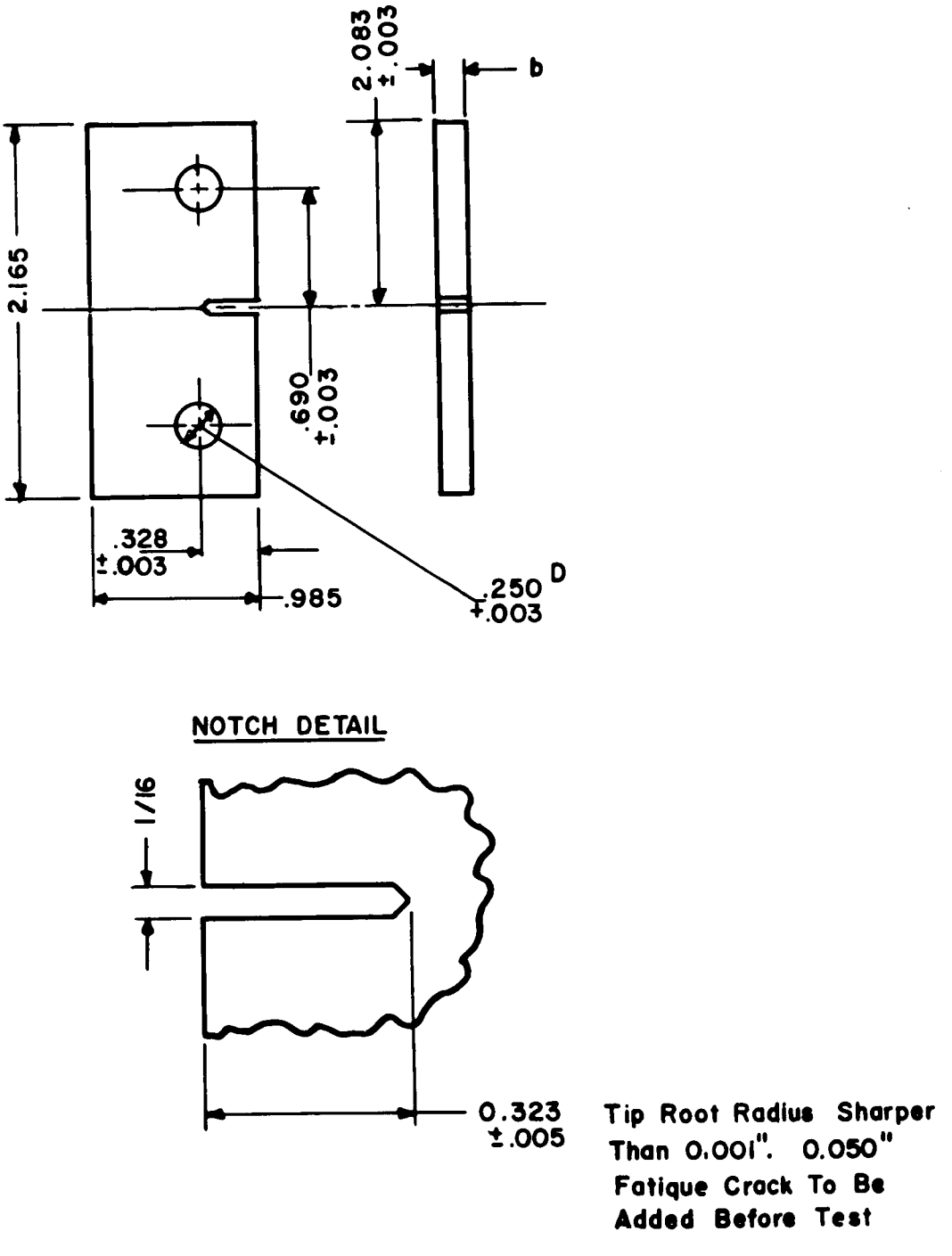

Figure 4. Single-edge Notched Specimen

Experimental Techniques

The notched bend specimens were machined with a notch root radius of 0.001 inch, maximum. Although under certain circumstances, this radius would be sufficiently sharp, most conditions require the use of a sharper notch or, preferably, a fatigue crack. Consequently, the notched bend specimens were precracked in fatigue using a special machine developed by Man-Labs, Inc., for this purpose. This equipment is shown in Figure 5.

After precracking, strain gages were attached to the notched bend specimens immediately ahead of the fatigue crack tip. The techniques used were modeled after those described by Kaufman[13] for cryogenic strain gage applications.

For those tests conducted at ambient temperature and -110° F, the surface of the specimens was cleaned by light sandblasting. Small high-elongation epoxy-backed "advance" strain gages were cemented in place using GA-5 cement. After curing and attaching the lead wires, a thin over-coating of GA-5 cement was sprayed over the gage assembly to provide mechanical protection. A slightly different technique was employed for specimens tested at -320° and -423° F. The surface of the specimens was cleaned by light sandblasting. A thin base coat (0.001 inch thick) of GA-5 cement was applied to the specimen by means of an air brush. After curing the base coat, a second thin layer of GA-5 cement was applied to the specimen by means of an air brush, and a small backless nichrome strain gage was embedded in the cement. The cement was then cured. After soldering the lead wires, a thin protective coating of GA-5 cement was applied to the strain gage installation.

The mechanical testing was conducted on an Instron tensile testing machine and is shown in detail in Figure 6. The notched bend specimens were tested in three-point loading. The end loads were reacted against a compression column which was attached to the moveable crosshead of the Instron. The central load was applied by means of a tension bar and loading saddle, which pass up the center of the compression column and are attached to the load cell of the Instron. The loading was accomplished by driving the moveable crosshead of the Instron downward.

For the tests conducted at ambient temperature, the specimens were broken in air at approximately 70° F. Tests at -110° and -320° F were conducted by immersing the compression column, specimen, and associated apparatus in a mixture of dry ice and alcohol and in liquid nitrogen, respectively.

Since it was not practical, from a safety standpoint, to use liquid hydrogen in the laboratory, a system had to be developed whereby testing could be accomplished at -423° F. The method devised utilized the evaporating gas of liquid helium (-452° F) as the cryogenic medium. The cold

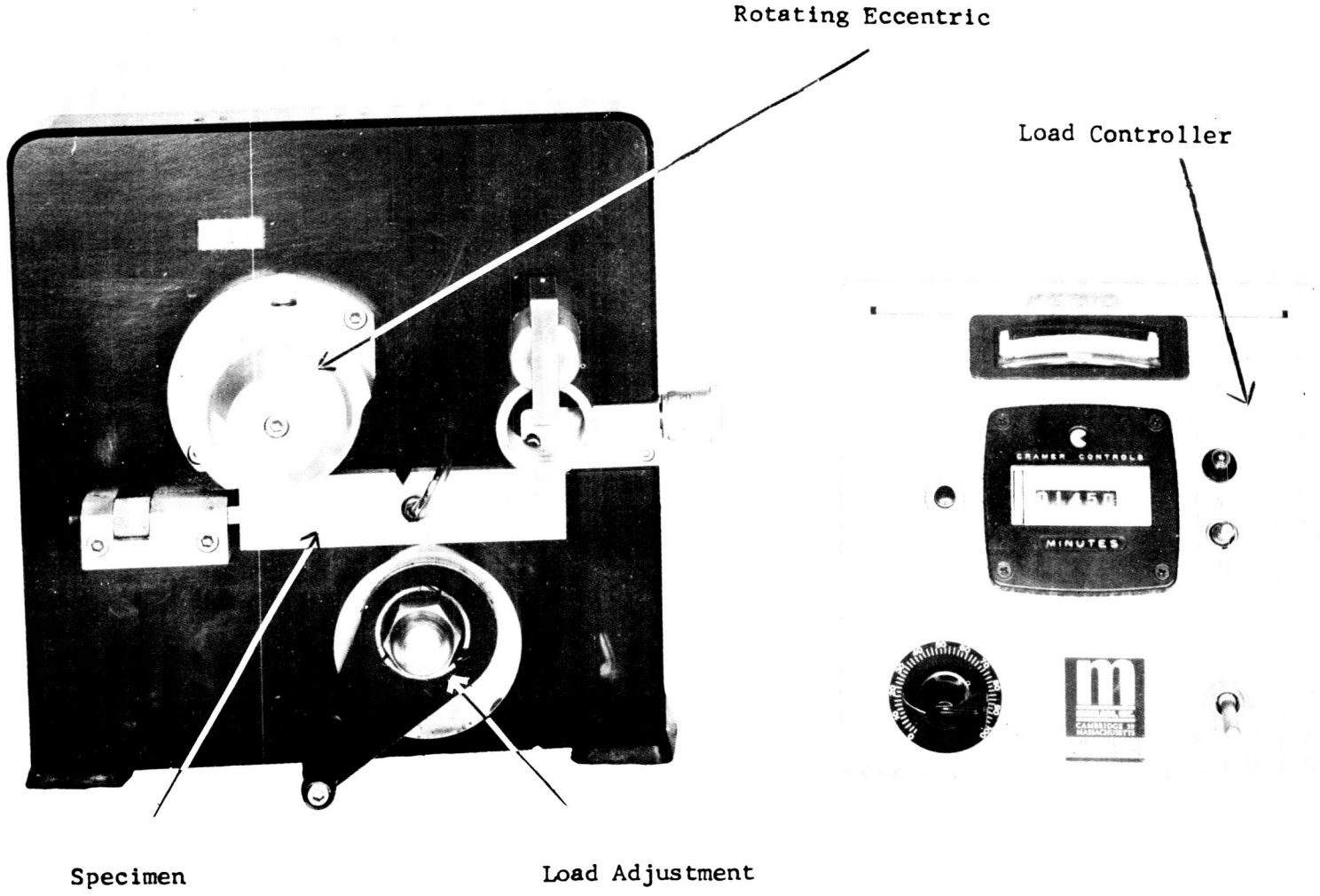

Figure 5. Fatigue Precracking Equipment

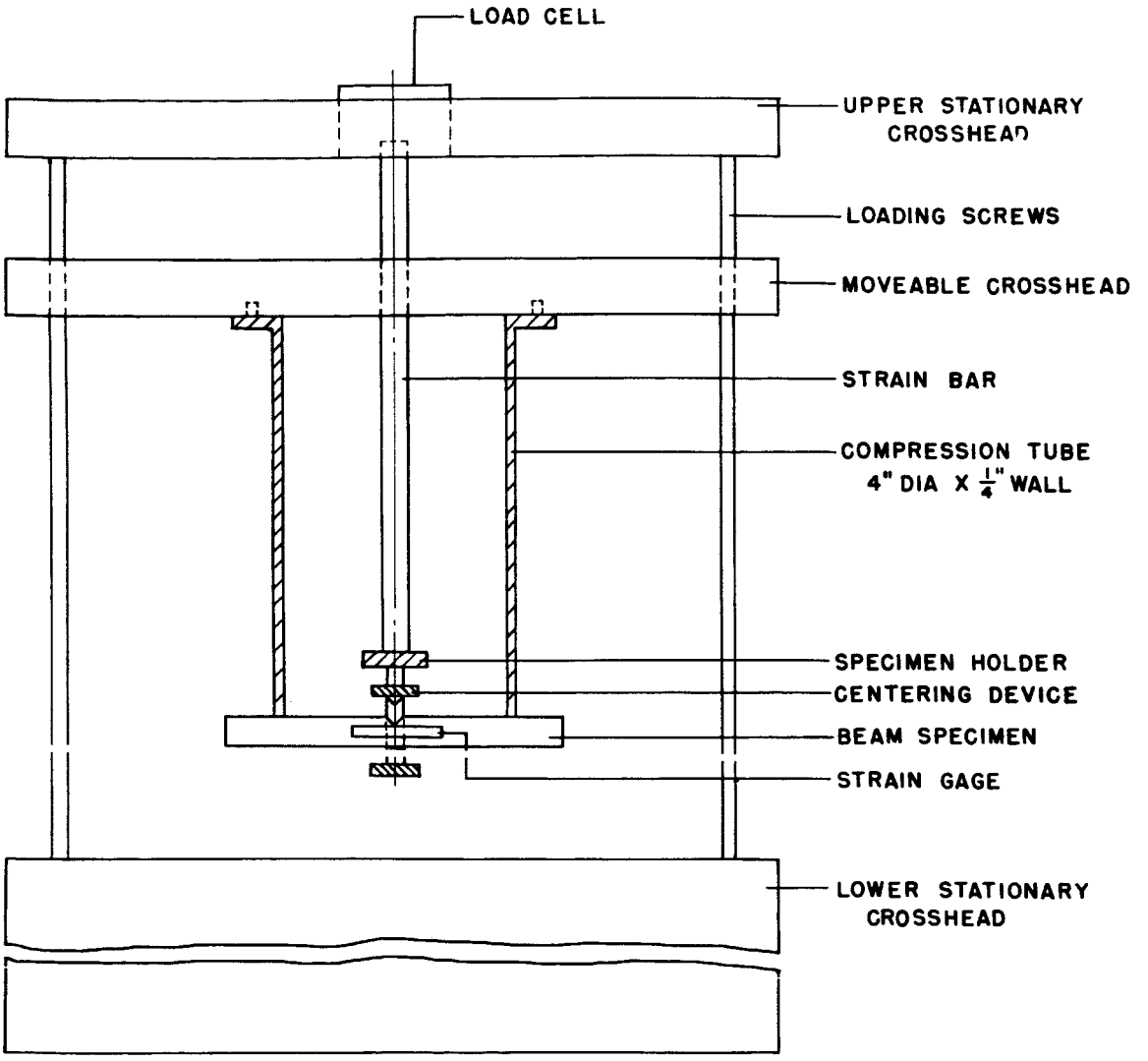

Figure 6. Schematic of Loading Notched Bend Specimens in Instron Test Machine

gas passed over an electrical resistance heater controlled so that the emerging stream of heated gas maintained the test specimen at liquid hydrogen temperature. A schematic of the cryostat and associated apparatus used is shown in Figure 7.

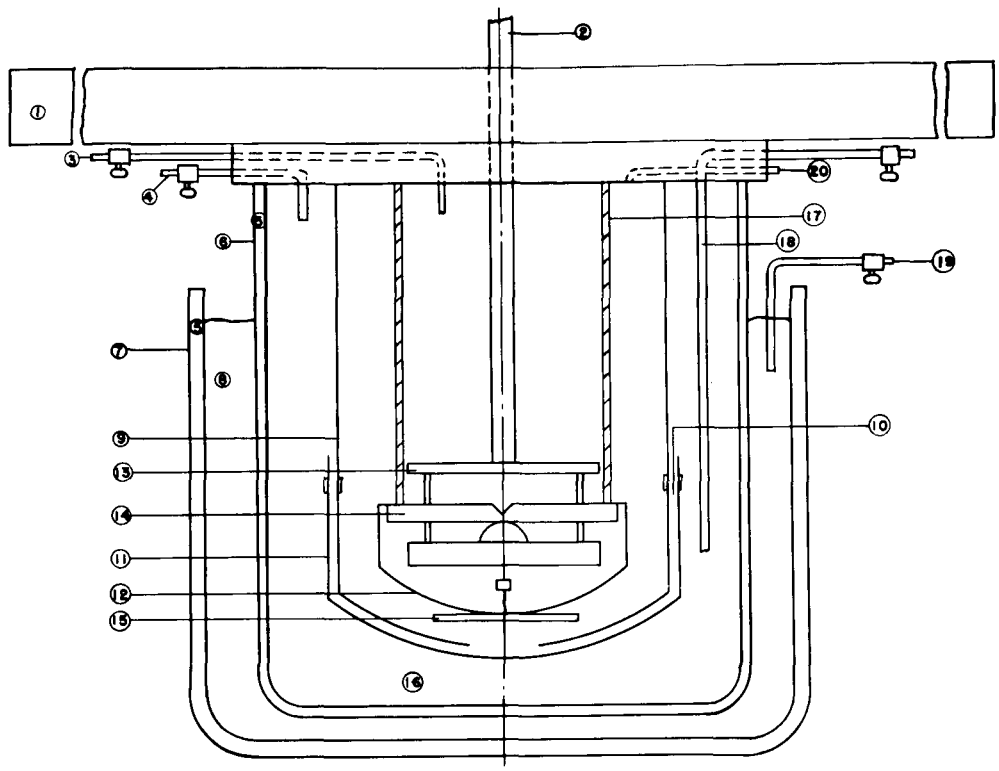

1. Moveable Crosshead
2. Strain Bar
3. Exhaust - Helium
4. Exhaust - Nitrogen & Helium
5. Vacuum
6. Inner Glass Dewar Flask
7. Outer Glass Dewar Flask
8. Liquid Nitrogen
9. Glass Cold Finger
10. Helium Gas Downflow Area
11. Outer Cup - Cold Finger
12. Wire Mesh Cage for Heater & Thermistor
13. Specimen Holder
14. Beam Specimen
15. Heater, Thermistor & Specimen Thermocouple
16. Liquid and/or Gaseous Helium
17. Steel Compression Tube
18. Liquid Helium Inlet
19. Liquid Nitrogen Inlet
20. Amphenole Plug for Instrumentation Lead Wires

Figure 7. Schematic of Cryostat and Associated Apparatus used for Tests Conducted at -423° F

A brief description of the operation of the cryostat follows. After placing the specimen in position in the holder, making all electrical connections, and sealing the cryostat to the testing machine, liquid nitrogen is introduced into the outer dewar until the proper level is maintained. This serves as a shield for the liquid helium system. Liquid nitrogen is then slowly introduced through inlet (18) * into the inner dewar and allowed to boil. The boil-off gas fills the region (16) and then drops down into cup (11) through opening (10) . The gas then travels up through the opening at the bottom of the cold finger (9) , over the heater and thermistor, over the specimen and out the exhaust (3) . Excess pressure is bled off by exhaust valve (4) . Cooling with liquid nitrogen is continued until the specimen temperature is approximately -250° F. The system is now purged with helium gas and liquid helium is transferred into the inner (area 16) dewar. The path of the cold helium gas is the same as that of the nitrogen gas. However, when the temperature of the cold helium gas stream is below -423° F, the heater coil is energized to condition the gas stream to liquid hydrogen temperature. The temperature of the specimen is confirmed by means of an attached differential thermocouple, shown in Figure 8.

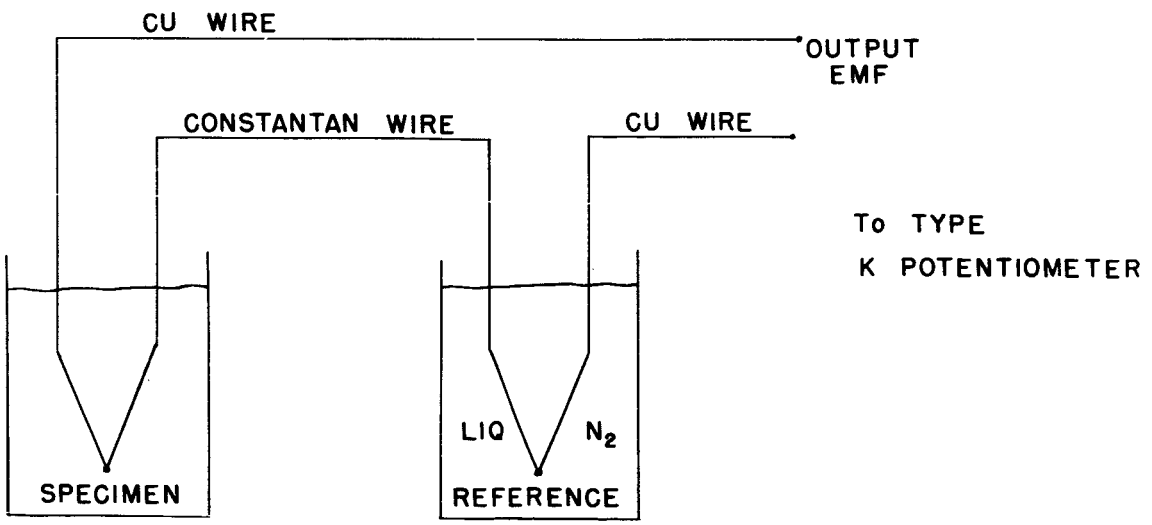

Figure 8. Schematic of Differential Thermocouple Circuit Used to Measure Cryogenic Temperatures

*Numbers in circles refer to Figure 7.

The differential thermocouple measures the absolute electromotive force generated between the cold junction (specimen) and reference temperature (liquid nitrogen). For accuracy in measuring these small voltages, a Leeds and Northrup type K potentiometer with a light beam ballistic galvanometer was used in conjunction with a copper-constantan thermocouple. The specimen is maintained at temperature for ten minutes prior to testing.

Experimental Results and Discussion

One-quarter Inch Thick 5Al-2.5Sn ELI Titanium Alloy Plate

Engineering Tensile Properties

Generalized typical engineering stress-strain curves for this material tested at ambient temperature, -110°, -320°, and -423° F are shown in Figure 9. The tensile tests at -423° F showed a different behavior from those at other temperatures and this is illustrated by the saw-toothed type curve shown in Figure 10. This behavior is characteristic of a material where a large portion of the plastic flow can be attributed to twinning, rather than slip.[14]

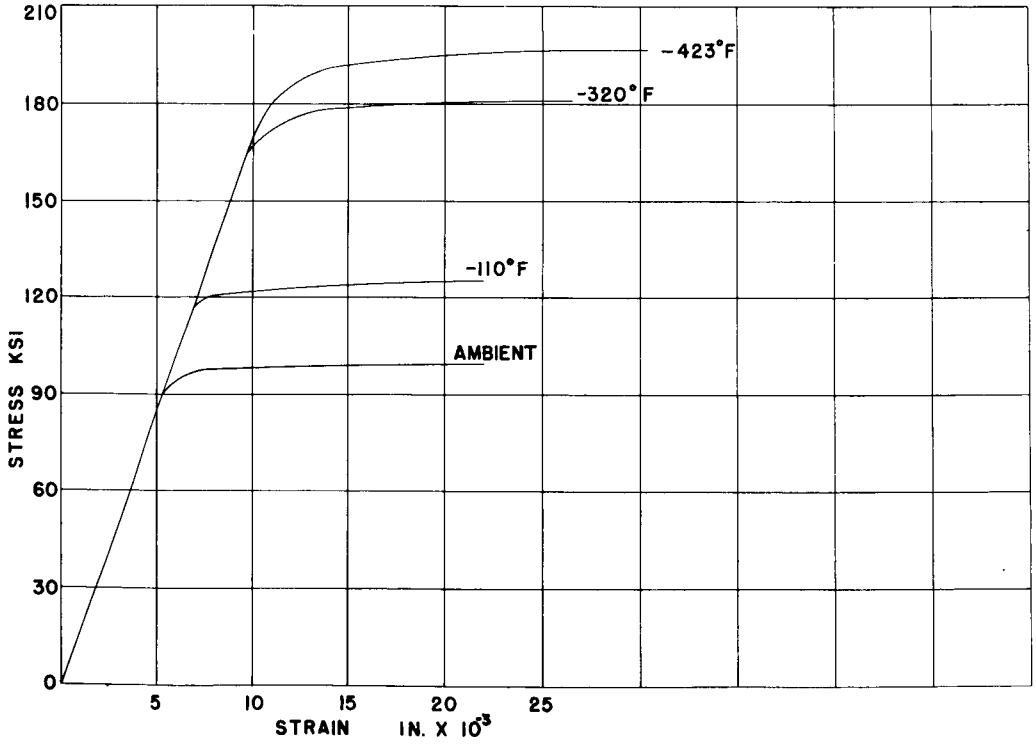

Figure 9. Stress-Strain Curves for 5Al-2.5Sn ELI Titanium Alloy as a Function of Testing Temperature

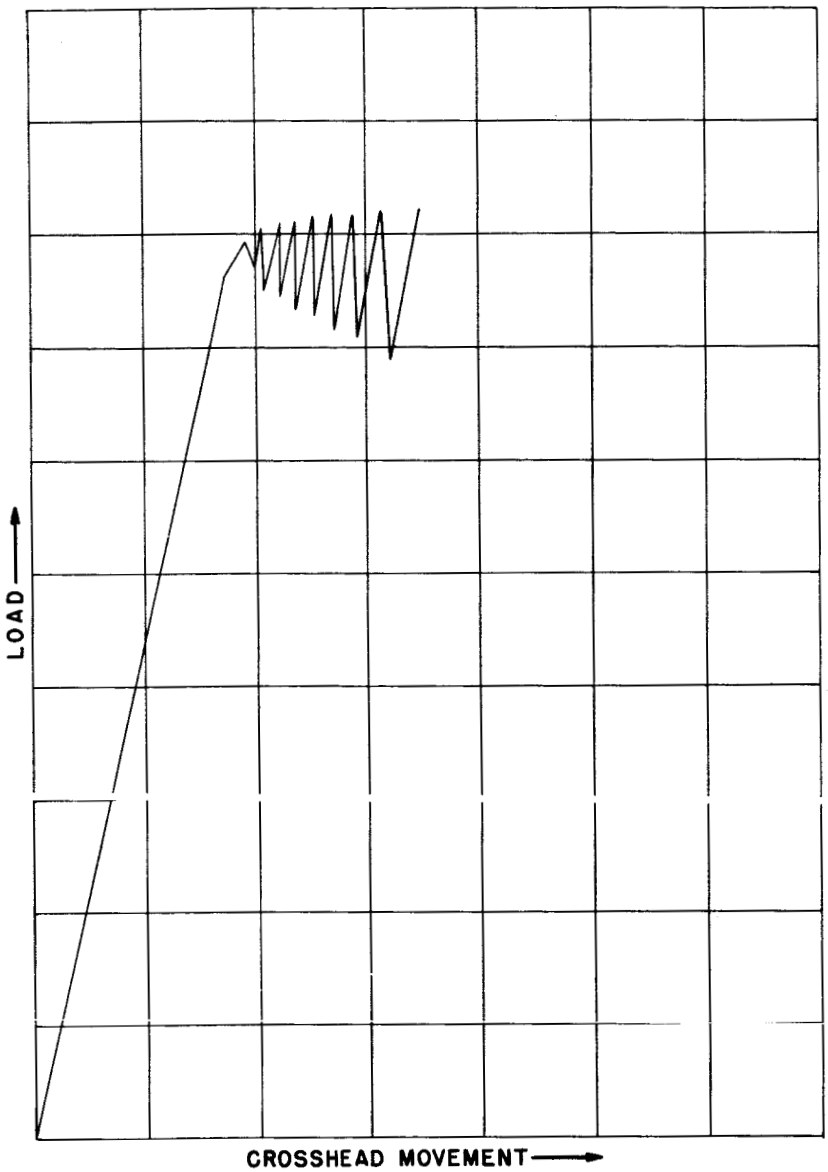

Figure 10. Load-Deflection Curve for 5Al-2.5Sn ELI Titanium Alloy tested at -423° F

This transition from slip to twinning may occur in close-packed metals with decreasing test temperature. The rapid unloading of the specimen is caused by the increased compliance of the specimen due to twinning. Since twinning is a very rapid process (order of microseconds) as contrasted with slip (order of milliseconds), the crosshead of the tensile machine cannot keep pace with the deformation of the specimen, so an unloading behavior is observed. The tensile data for both the longitudinal and transverse specimens are summarized graphically in Figure 11 and tabulated in Table III.

TABLE III

Tensile Properties of 1/4 Inch 5Al-2.5Sn ELI Titanium Alloy Plate as a Function of Testing Temperature

Direction	Specimen No.	Test Temp (°F)	Strength (psi) Yield, at 0.20% Offset	Strength (psi) Tensile	Reduction of Area (%)	Elongation (%)	Strain Hardening Exponent, n
Longitudinal	1	Ambient	102,000	116,250	42.6	24.4	0.080
Longitudinal	2	"	100,000	114,500	41.3	25.3	0.071
Transverse	1	"	105,500	116,000	42.6	23.1	0.052
Transverse	2	"	102,400	114,000	38.7	25.3	0.074
Longitudinal	1	-110	126,000	132,400	39.7	24.0	0.058
Longitudinal	2	-110	-	-	-	-	-
Transverse	1	-110	126,000	131,100	35.8	22.2	0.047
Transverse	2	-110	130,500	133,600	35.8	21.3	0.037
Longitudinal	1	-320	-	177,000	34.8	23.6	-
Longitudinal	2	-320	170,500	181,400	32.8	-	-
Transverse	1	-320	174,500	181,400	35.8	22.7	-
Transverse	2	-320	-	184,300	34.8	24.2	-
Longitudinal	1	-423	195,500	225,000	25.5	12.0	-
Longitudinal	2	-423	-	222,100	23.5	14.7	-
Transverse	1	-423	187,500	203,000	21.3	29.9	-
Transverse	2	-423	174,500	181,400	19.1	31.9	-

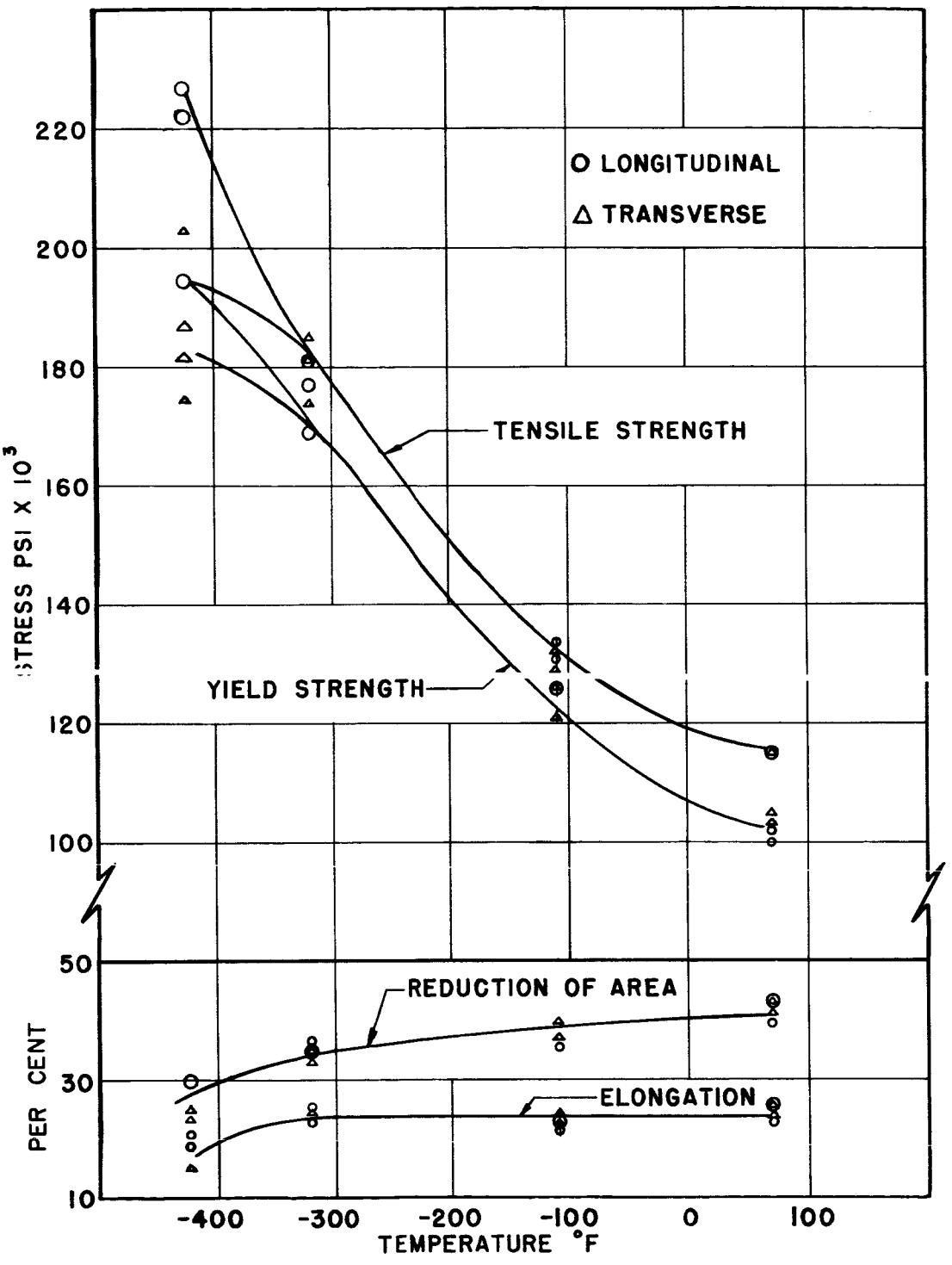

Figure 11. Tensile Properties of 1/4 inch thick 5Al-2.5Sn ELI Titanium Alloy Plate as a Function of Testing Temperature

Since twinning is the primary mode of deformation, it is desirable to further study this phenomenon.

Metallographic specimens were taken of the plastically deformed areas of the tensile specimens. The structures observed are shown in Figures 12, 13, 14, and 15. Examination of these structures shows some evidence of twinning, together with slip. As the testing temperature is lowered, the number of twins in the structure increases. At -423° F, the plastic deformation mechanism is primarily by twinning.

This material exhibits a high degree of sensitivity of strength to temperature and shows an increase of yield strength from 100,000 psi at room temperature to over 200,000 psi at -423° F. The increase was accomplished with only a minor loss in the commonly accepted ductility parameters, namely elongation and reduction of area.

No high degree of anisotropy was observed in the ordinary engineering tensile properties, as shown by uniformity of results between the longitudinal and transverse specimens (Table III).

Plane Strain Fracture Toughness

The plane strain fracture toughness values determined using the 1/4 inch thick notched bend specimens and small single-edge notched specimens (SEN) in both the longitudinal and transverse directions are shown as a function of testing temperature in Figure 16. The experimental data are summarized in Table IV. Comparison of the plane strain fracture toughness values computed by the compliance equation and Bueckner's equation shows that the latter gives significantly higher values. This is in contrast to data reported in Reference 11. However, those observations were made using relatively large specimens, whereas this investigation is concerned with quite small specimens.

It will be observed that the fracture toughness values determined at room temperature and -110° F are indicated as lower bound values only. In these tests, the load-deflection curves showed a gradual departure from linearity and did not give a pronounced pop-in point. Under these conditions it is possible to estimate the pop-in load and, therefore, the plane strain fracture toughness by extending the linear portion of the load-deflection curve and drawing a tangent to the sloping portion, as shown in Figure 17. The pop-in is arbitrarily defined as the intersection of these two lines.

In regard to the adequacy of the specimen and testing technique, the following points should be considered. As mentioned previously, Kies et al[12] have shown that for valid K_{Ic} measurements in notched bending, the nominal stress at the root of the notch should not exceed 1.1 times the yield strength. Calculating this stress,

Neg: 36.231.S125/AMC.65

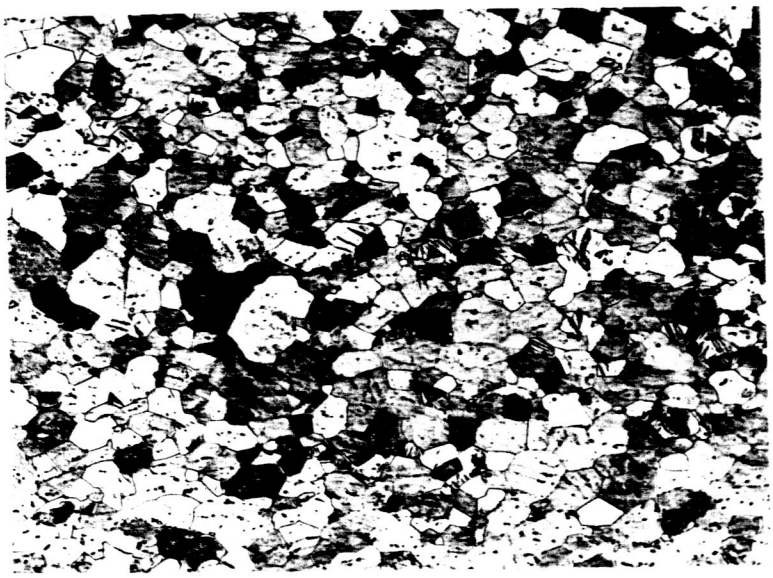

100X

500X

Figure 12. Structure of Plastically Deformed Area of Tensile Specimen of 5Al-2.5Sn ELI Titanium tested at Ambient Temperature
Etchant: ethylene glycol and 10% HF, electrolytic

Neg: 36.231.S126/AMC.65

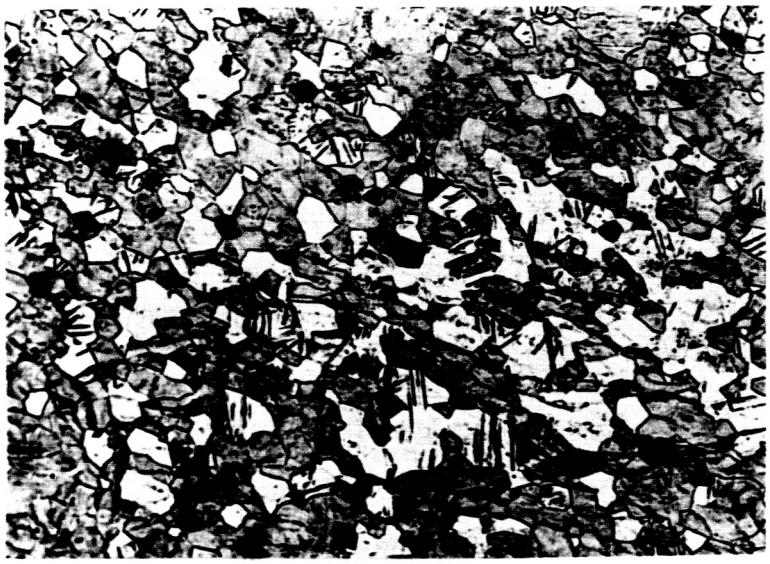

100X

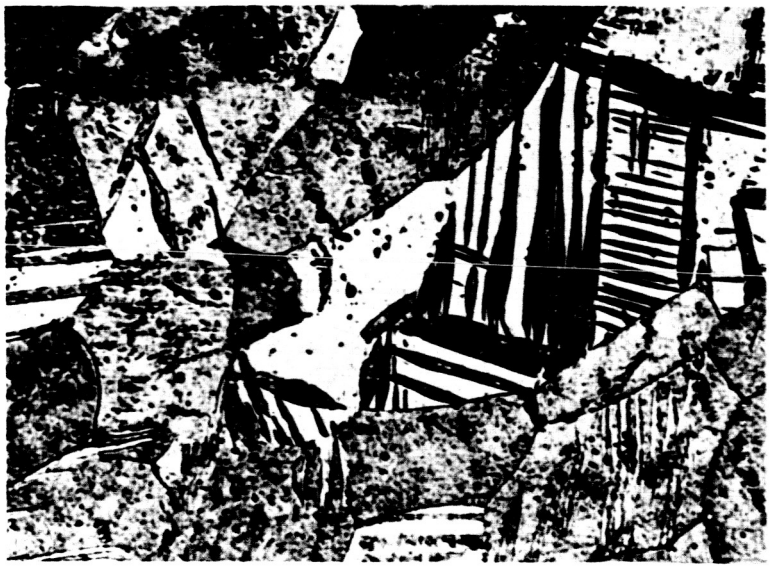

500X

Figure 13. Structure of Plastically Deformed Area of Tensile Specimen of 5Al-2.5Sn ELI Titanium tested at -110° F

Etchant: ethylene glycol and 10% HF, electrolytic

Neg: 36.231.S127/AMC.65

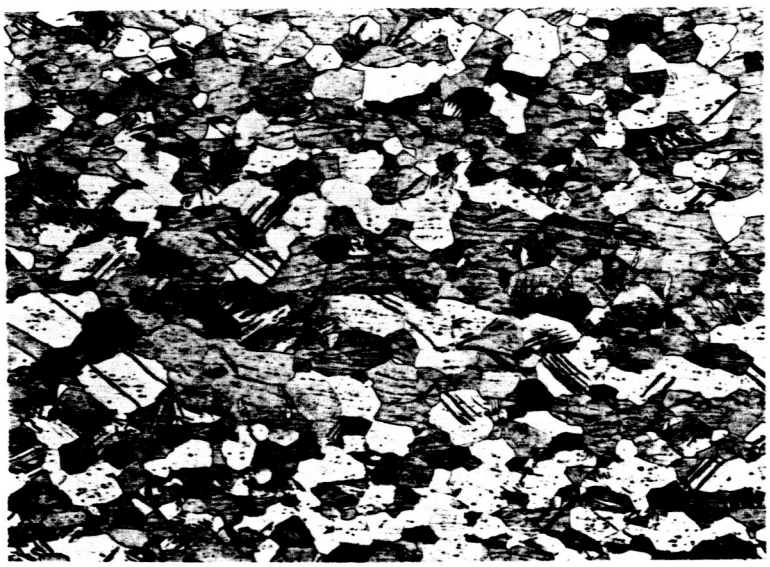

100X

500X

Figure 14. Structure of Plastically Deformed Area of Tensile Specimen of 5Al-2.5Sn ELI Titanium tested at -320° F

Etchant: ethylene glycol and 10% HF, electrolytic

Neg: 36.231.S128/AMC.65

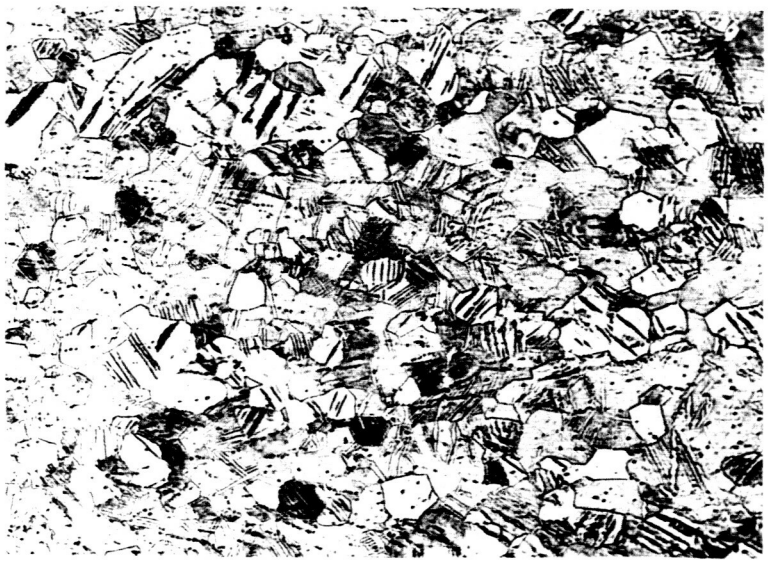

100X

500X

Figure 15. Structure of Plastically Deformed Area of Tensile Specimen of 5Al-2.5Sn ELI Titanium tested at -423° F

Etchant: ethylene glycol and 10% HF, electrolytic

TABLE IV
Plane Strain Fracture Toughness Properties of
1/4 inch 5Al-2.5Sn ELI Titanium Alloy Plate
as a Function of Testing Temperature

Testing Temperature (°F)	P (lb)	a (in.)	K_{Ic} (psi $\sqrt{in.}$) Compliance Equation	K_{Ic} (psi $\sqrt{in.}$) Bueckner's Equation	Breaking Load (lb)
		Longitudinal			
80	476	0.182	35,900*		870
	480	0.153	30,900*		1110
	685	0.154	42,800*		965
-110	995	0.095	45,200*		1460
	770	0.135	44,300*		1120
	880	0.122	46,800*		1030
-320	820	0.148	50,600	62,000	820
	855	0.140	50,700	61,400	865
	830	0.150	52,200	63,200	830
-423	863	0.127	47,500	56,400	863
	775	0.117	40,000	54,000	828
	702	0.143	42,700	51,600	750
		Transverse			
80	588	0.176	43,200*		940
	633	0.159	42,500*		1080
	665	0.131	37,700*		1140
-110	780	0.148	48,900*		1065
	770	0.142	46,800*		1060
	740	0.153	48,000*		1000
-320	800	0.132	45,400	49,300	800
	815	0.135	47,400	57,200	815
	800	0.141	48,100	58,000	800
-423	621	0.1561	40,900	48,800	675
	660	0.1466	41,100	49,800	765
	490	0.1700	34,800	41,800	690

*Lower bound values.

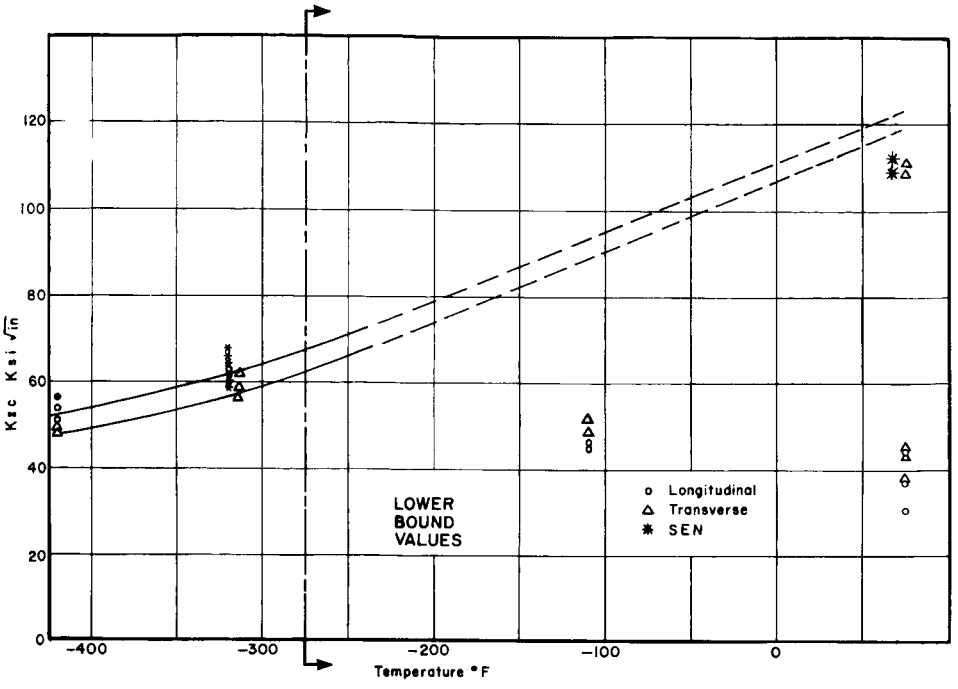

Figure 16. Variation of the Plane Strain Fracture Toughness of 1/4 inch thick 5Al-2.5Sn ELI Titanium Alloy Plate as a Function of Testing Temperature

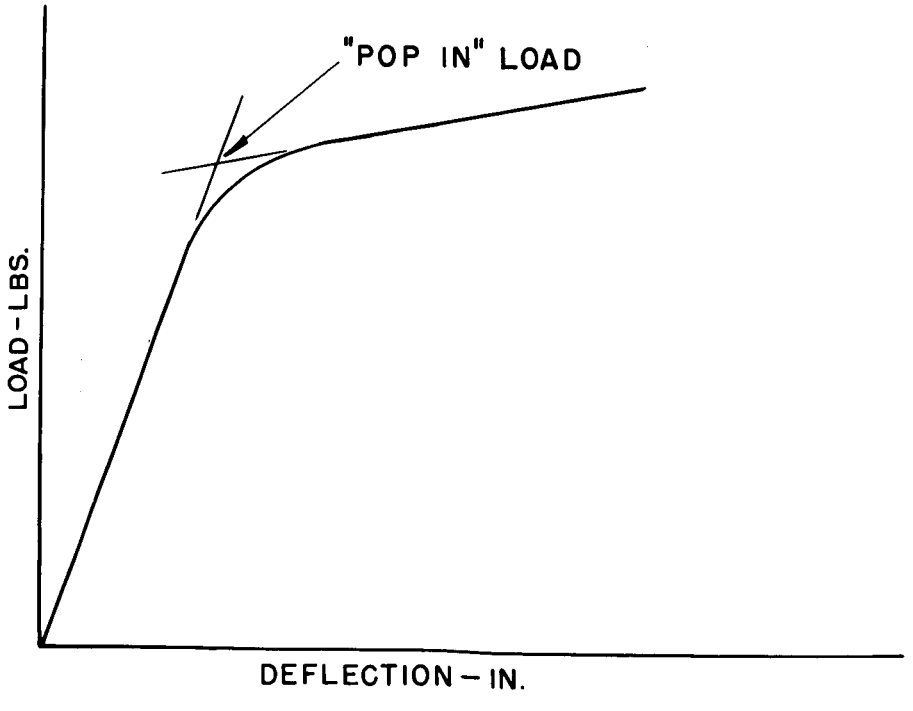

Figure 17. Method of Estimating Pop-in Load by Tangent-Intercept Technique

$$\sigma_{nom} = \frac{3M}{B\alpha^2 d2} \qquad (11)$$

and using the data in Table IV showed that σ_{nom} exceeded the maximum allowable for all tests conducted at room temperature and at -110° F. Previous experience with specimens having high nominal stresses shows that under these conditions, the K_{Ic} values determined are depressed. The plane strain fracture toughness values so determined are arbitrarily defined as lower bound values.

To gain additional insight into the behavior of this material, some reasonable estimate of the K_{Ic} value at room temperature is needed. Srawley[15] has shown that the single-edge notched specimen has the greatest measuring capacity in terms of K_{Ic} of all the various specimen geometries discussed. Consequently, small single-edge notched specimens were machined from the 1/4 inch thick plate in both the longitudinal and transverse directions, and tested at room temperature. The load-deflection curves did not show a marked "pop-in" point, but exhibited a gradual departure from linearity. The point of departure from linearity was arbitrarily selected to compute the plane strain fracture toughness. These data are summarized in Table V and are also shown on Figure 16.

TABLE V
Single-edge Notch Fracture Toughness Values
for 1/4 inch 5Al-2.5Sn ELI Titanium Alloy Plate
at Room Temperature

Spec No.	Crack Depth (in.)	Load (lb) Pop-in	Load (lb) Max	Stress (psi) Pop-in	Stress (psi) Max	K_{Ic} (psi $\sqrt{in.}$) Uncorrected	K_{Ic} (psi $\sqrt{in.}$) Plastic Zone Corrected
				Longitudinal			
1	0.387	5500	7330	20,900	28,100	79,200	100,200
2	0.394	5300	7100	20,300	27,200	78,800	100,900
				Transverse			
1	0.402	5400	6650	20,800	25,600	82,800	111,000
2	0.378	5880	7330	22,700	28,300	82,800	108,700
3	0.372	5750	7590	22,200	29,300	79,800	101,500

In high stress tests, it is customary to correct for the effect of the plastic strain at the crack tip. The plastic deformation relaxes the stress so that a slightly lower value of plane strain fracture toughness is calculated. This effect is taken into consideration by the addition of a small increment equal to the radius of the plastic strain zone to the measured crack length. Examination of the data in

this table shows that the plastic zone correction results in a relatively large change in the plane strain fracture toughness (approximately 20 percent) and indicates that the plastic zone size is not small compared with the crack length. Therefore, these corrected values are considered reasonable estimates of minimum K_{Ic} of this material. It will be noted that these minimum estimates of K_{Ic} are considerably larger than the lower bound values determined using the small notched bend specimen.

To obtain valid pop-in data, it has been shown that the plate thickness should be equal to or greater than four times the radius of the plastic zone size.[7] This is expressed mathematically as

$$B = 4r_{ys} = \frac{2K_{Ic}^2}{\pi\sigma_{ys}^2} \tag{12}$$

Solving this equation with B equal to 1/4 inch and a yield strength equal to 100,000 psi gave a maximum determinable value for K_{Ic} of 62,600 psi $\sqrt{\text{in.}}$ for pop-in to occur. This is considerably less than the estimated minimum value of 100,000 psi $\sqrt{\text{in.}}$ as determined using the single-edge notched specimens. This analysis may now be extended to the tests conducted at -320° F. Solution of Equation 12 using the 1/4 inch thick specimen and a yield strength of approximately 170,000 psi gave a maximum determinable value of K_{Ic} of 106,000 psi $\sqrt{\text{in.}}$ The value of K_{Ic} determined at this temperature is much less than the maximum value.

The final point to be considered is the depth of the beam. It has been stated for sheet testing[7] that the width of the specimen should be 20 times the plastic zone size. The same conditions should apply to the notched bend specimens in that the beam depth should be 20 times the plastic zone size. Calculation of the plastic zone size at room temperature gave a value of 0.159 inch, or a minimum beam depth of 3.180 inches. This minimum value of beam depth is considerably greater than the 0.500 inch used. Extending this analysis to tests conducted at -320° F gave a value of 0.0233 inch for the radius of the plastic zone, or a minimum value for the beam depth of 0.466 inch (which is less than the 0.500 inch beam depth employed). Gross[8] has stated that the limit of applicability of the specimen will be reached if the nominal stress at the crack tip reaches the yield stress of the material, as stated in

$$\frac{6M}{B(d-a)^2} = \sigma_{ys} \tag{13}$$

Solution of this equation, using data obtained at -320° F, gave a value of d-a equal to 0.410 inch. Therefore, the 0.500 inch deep beam should be adequate.

The data at -423° F show an increasing value of yield strength with a decrease in toughness, so that those specimens which are adequate at -320° F will be adequate at -423° F.

These calculations show the small notched bend specimens should give reliable data at -320° F. Therefore, the use of another specimen geometry to measure the plane strain fracture toughness would supply supporting data. Small single-edge notch specimens (Figure 4) were machined from the 1/4 inch plate in the longitudinal and transverse directions. These specimens were precracked in fatigue and instrumented with strain gages to detect the pop-in load. The plane strain fracture toughness calculated from these experiments, conducted at -320° F, are plotted in Figure 16 and are summarized in Table VI. Comparison of the plane strain fracture toughness values determined by the single-edge notched specimens and the bend specimens using Beuckner's solution shows that both specimens give essentially the same value of fracture toughness.

TABLE VI
Plane Strain Fracture Toughness of
5Al-2.5Sn ELI Titanium Plate
Using Single Edge Notched Specimens at -320° F

Spec No.	a (in.)	Load (lb)	Stress (psi)	K_{Ic} (psi $\sqrt{in.}$) Uncorrected	K_{Ic} (psi $\sqrt{in.}$) Plastic Zone Corrected
			Transverse		
2/8-1	0.3715	3935	15,800	56,500	60,900
2/8-2	0.3706	4220	17,200	61,500	66,000
2/8-3	0.4004	3400	13,830	55,000	58,600
2/8-4	0.3415	4560	18,550	60,200	64,000
			Longitudinal		
2/8-3	0.3487	4240	17,300	57,200	61,000
2/8-4	0.3488	4490	18,300	61,000	64,600
2/9-5	0.3576	4355	17,750	60,300	64,500
2/9-6	0.3674	4420	17,960	62,700	67,900

One-half Inch Thick 5Al-2.5Sn ELI Titanium Alloy Plates

Engineering Tensile Properties.

The engineering tensile properties of this material are plotted as a function of testing temperature in Figure 18 and the data are summarized in Table VII. Essentially the same comments are pretinent regarding these data as for the data obtained from the 1/4 inch plate.

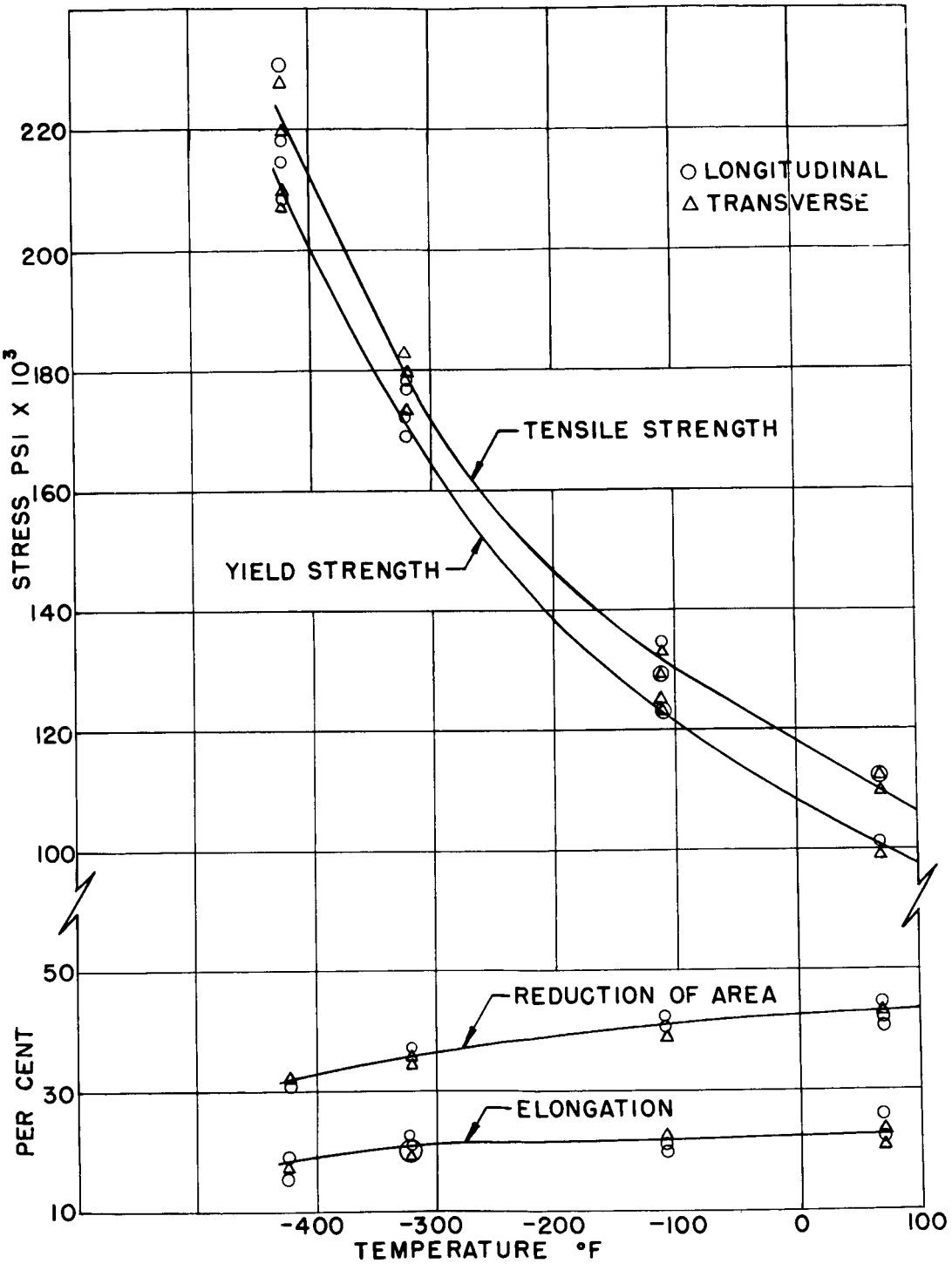

Figure 18. Tensile Properties of 1/2 inch thick 5A1-2.5Sn ELI Titanium Alloy Plate as a Function of Testing Temperature

TABLE VII

Tensile Properties of 1/2 Inch 5Al-2.5Sn ELI Titanium Alloy Plate as a Function of Testing Temperature

Direction	Specimen No.	Test Temp (°F)	Strength (psi) Yield, at 0.20 Offset	Strength (psi) Tensile	Reduction of Area (%)	Elongation (%)	Strain Hardening Exponent, n
Longitudinal	1	Ambient	99,000	110,000	42.6	23.6	0.067
Longitudinal	2	"	101,000	112,500	43.9	22.7	0.067
Transverse	1	"	101,000	112,500	41.9	23.1	0.056
Transverse	2	"	101,000	112,500	43.8	26.2	0.068
Longitudinal	1	-110	123,800	133,500	42.1	22.6	0.048
Longitudinal	2	-110	125,300	128,900	38.7	22.2	0.050
Transverse	1	-110	-	134,000	40.5	21.3	-
Transverse	2	-110	124,000	128,700	38.7	20.0	0.054
Longitudinal	1	-320	177,000	182,900	36.1	20.0	0.0603
Longitudinal	2	-320	173,000	182,750	34.8	21.3	-
Transverse	1	-320	169,500	178,500	36.5	20.0	-
Transverse	2	-320	172,500	179,300	37.1	22.7	-
Longitudinal	1	-423	202,500	215,000	31.9	16.9	-
Longitudinal	2	-423	208,500	218,300	31.2	19.1	-
Transverse	1	-423	208,000	219,400	31.8	-	-
Transverse	2	-423	210,000	228,000	31.2	17.8	-

Plane Strain Fracture Toughness

Of interest to the investigator and practical importance to the designer is the possible variation of the plane strain fracture toughness with respect to crack orientation. In this thicker plate it is possible to study the anisotropy of the material with respect to the plane strain fracture toughness. The orientation of the various specimens is shown in Figure 19, in which the L and T designations give the orientation of the specimens relative to the rolling direction of the plate. In the S series of specimens, the direction of crack propagation is parallel to the rolling plane; in the D series, the specimens are so oriented that the path of crack propagation is perpendicular to the rolling plane.

The plane strain fracture toughness values are plotted as a function of testing temperature in Figures 20 and 21, and are summarized in Table VIII. The same limitations prevailed in these tests as in those described for the 1/4 inch thick plate. Consequently, all tests conducted at ambient temperature and -110° F, using the small notched bend specimens, are considered lower bound values.

In an attempt to obtain a more accurate measure of the plane strain fracture toughness of this material at ambient temperature and -110° F, larger notched bend bars were machined from the 1/2 inch thick plate. These specimens were 1/2 inch thick by 3/4 inch deep, with a four inch span. The load-deflection curves for these specimens showed no pronounced pop-in point, but exhibited a gradual departure from linearity, as did the small notched bend specimens. Consequently, the values determined are also indicated as lower bound. These values are also plotted in Figure 20.

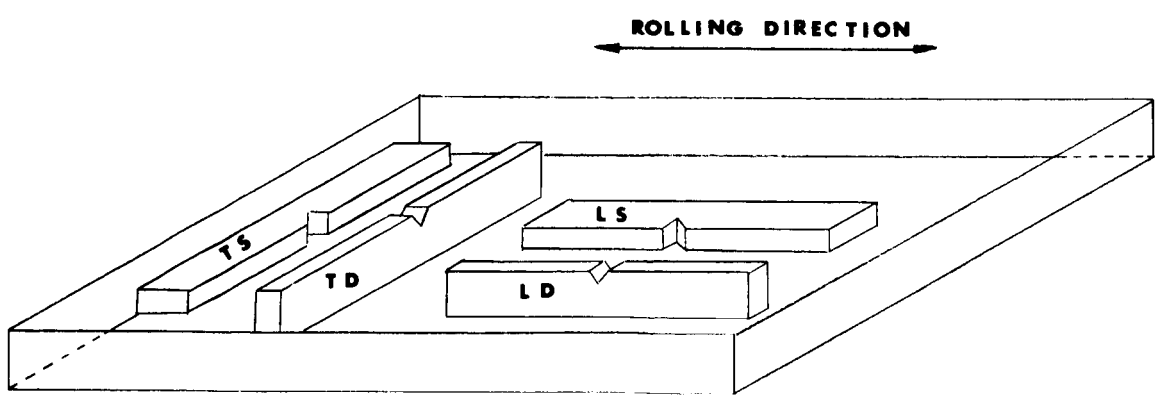

Figure 19. Orientation of Specimens Machined from 1/2 inch thick Plate

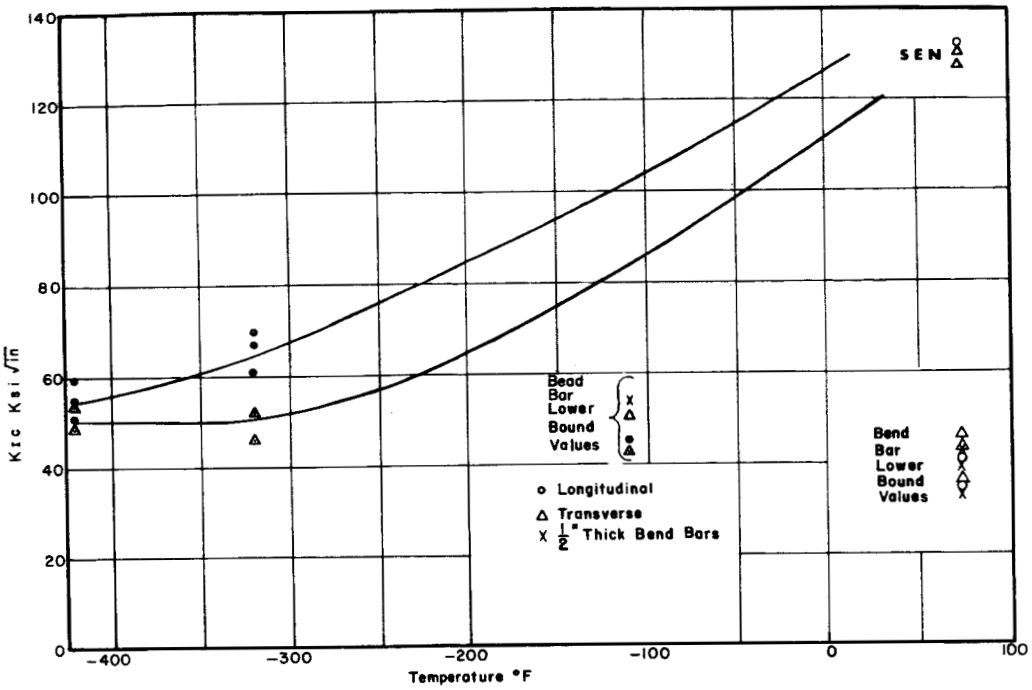

Figure 20. Variation of the Plane Strain Fracture Toughness of 1/2 inch thick 5Al-2.5Sn ELI Titanium Alloy Plate as a Function of Testing Temperature for LS and TS Specimen Series

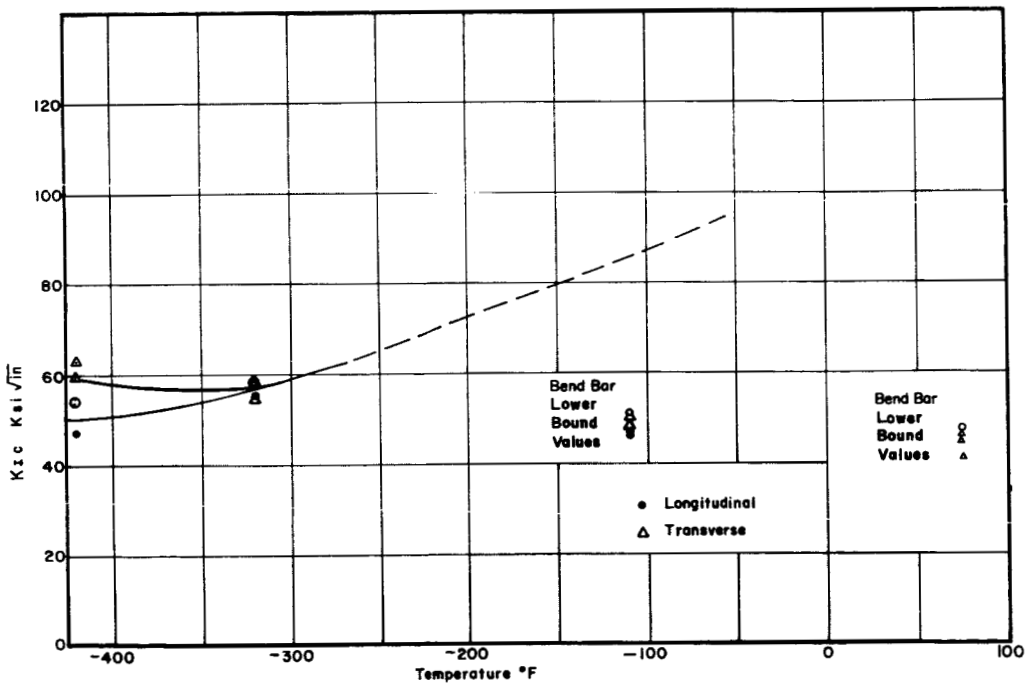

Figure 21. Variation of the Plane Strain Fracture Toughness of 1/2 inch thick 5Al-2.5Sn ELI Titanium Alloy Plate as a Function of Testing Temperature for LD and TD Specimen Series

TABLE VIII
Plane Strain Fracture Toughness Values of
1/2 inch 5Al-2.5Sn ELI Titanium Alloy Plate
(Notched Bend Specimens)

Testing Temperature (°F)	P (lb)	a (in.)	K_{Ic} (psi $\sqrt{in.}$) Compliance Equation	K_{Ic} (psi $\sqrt{in.}$) Bueckner's Equation	Breaking Load (lb)
		Longitudinal - LS			
80	735	0.1003	37,100*		1140
	830	0.1045	42,300*		1185
	845	0.0992	41,600*		1210
-110	875	0.1017	45,200*		1285
	900	0.1032	45,700*		1310
-320	1190	0.0983	59,100	67,000	1190
	1230	0.0986	60,300	69,800	1230
	1070	0.0987	50,600	60,800	1150
-423	912	0.0980	44,900	51,400	912
	1055	0.0988	52,600	59,600	1055
	965	0.0980	47,700	54,400	965
		Longitudinal - LD			
80	920	0.1021	47,900*		1110
	880	0.1067	47,300*		1125
	890	0.1107	46,900*		1105
-110	920	0.1099	48,300*		1290
	905	0.1074	46,800*		1205
	980	0.1076	50,800*		1230
-320	910	0.1090	48,500	55,200	1265
	980	0.1067	50,300	58,000	1010
	910	0.1129	47,500	55,000	1025
-423	890	0.1092	47,900	53,600	970
	970	0.0980	47,300	54,600	970
	780	0.1088	41,000	47,200	780

*Lower bound values.

Code: P - Load at "pop-in."
a - Crack length.

TABLE VIII (Cont'd)

Testing Temperature (°F)	P (lb)	a (in.)	K_{Ic} (psi $\sqrt{in.}$) Compliance Equation	K_{Ic} (psi $\sqrt{in.}$) Bueckner's Equation	Breaking Load (lb)
			Transverse - TS		
80	780	0.1054	40,000*		1185
	835	0.1085	46,200*		1195
	840	0.1153	45,200*		1230
-110	875	0.1266	51,300*		1160
	850	0.1061	43,100*		1380
	880	0.1024	43,700*		1390
-320	860	0.1131	46,400	52,800	890
	790	0.1054	40,200	46,400	975
	750	0.1312	54,800	51,500	750
-423	860	0.0997	43,100	48,800	885
	924	0.1054	46,800	54,000	960
	945	0.1012	54,700	54,200	945
			Transverse - TD		
80	865	0.1078	44,100*		1140
	865	0.1115	45,600*		1025
	810	0.1058	41,700*		1170
-110	885	0.1120	47,600*		1110
	885	0.1121	50,600*		1080
	950	0.1046	48,400*		1280
-320	950	0.1033	52,600	55,200	975
	995	0.1068	51,500	58,400	1320
	930	0.1076	48,200	54,200	1100
-423	1010	0.1110	53,100	60,000	1010
	1115	0.1025	56,200	63,600	1185
	985	0.1090	52,000	59,200	985

*Lower bound values.

Code: P - Load at "pop-in."
a - Crack length.

The determination of the plane strain fracture toughness at room temperature, while not essential in the development of design criteria, is important in developing the general trend of material behavior with temperature. The results obtained using the small single-edge notched specimens machined from 1/4 inch thick plate were sufficiently encouraging to warrant trying a larger specimen. Larger single-edge notched specimens (Figure 22) were machined from the 1/2 inch thick plate in both the longitudinal and transverse directions. These specimens were fatigue cracked, instrumented with strain gages to detect the pop-in, and broken at room temperature. The data are summarized in Table IX.

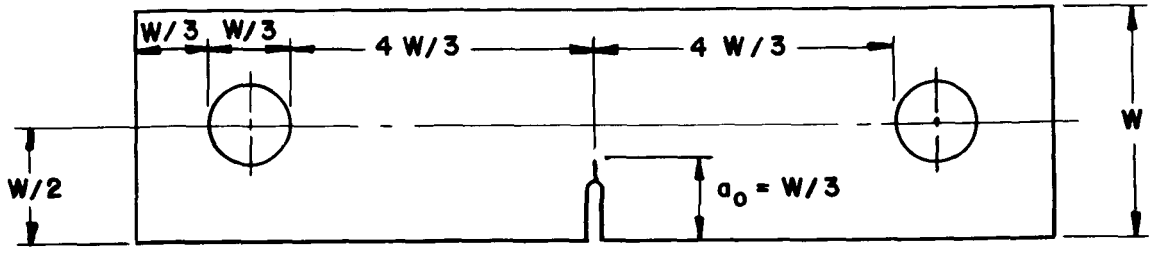

B = THICKNESS

$4 < W/B < 8$

Figure 22. Large Single-edge Notched Specimen

TABLE IX
Single-edge Notched Fracture Toughness Values for
1/2 Inch 5Al-2.5Sn ELI Titanium Plate at Room Temperature

Direction	Crack Depth (in.)	Maximum Load (lb)	K_{Ic} (psi $\sqrt{in.}$)
Longitudinal	0.568	37,500	131,800
	0.508	41,900	127,000
Transverse	0.526	41,000	130,000
	0.520	40,750	127,000

These data show that room temperature K_{Ic} values of approximately 130,000 psi $\sqrt{in.}$ (plotted in Figure 20) are quite reasonable. This figure shows that the K_{Ic} values are a function of the testing temperature. Such behavior would be anticipated, since an inverse first order dependency of K_{Ic} and yield strength exists. It will also be observed that the K_{Ic} for the TD series (specimen transverse to rolling direction, with crack propagating into the thickness direction of the plate) and TS (specimen transverse to rolling direction and crack propagation parallel to rolling plane) appear to remain constant as the testing temperature is reduced to -423° F. Tests for the LS and LD specimens show a decrease in plane strain fracture toughness

as the testing temperature is reduced to -423° F. This behavior may be related to preferred orientation and to the change in the mechanism of plastic deformation at liquid hydrogen temperatures.

BASIC DESIGN DATA - TEXTURE HARDENING

The textures of rolled sheets of hexagonal close packed (HCP) materials cause high yield strengths under biaxial tension, thus making some of these materials especially suitable for pressure vessels. Under combined stress loading, anisotropic continuum theory of yielding and plastic flow predict striking deviations from the vonMises criterion. In particular, the resistance of a sheet to thinning under stresses in its plane has much influence on the form of the two-dimensional yield locus, as discussed by Hosford and Backofen.[16]

One simple measure of the thinning resistance of sheet metal is the ratio, R, of the width strain to thickness strain found in the tension test on a strip. In an isotropic material, the width and thickness strains are equal, so R = 1. A particularly straightforward example is a balanced biaxial tension in the plane of a sheet. Such a stress system is equivalent to a uniaxial through-thickness compression plus a hydrostatic tension. Therefore, yielding under the balanced tension can occur only when the tensile stresses reach a value equal to the compressive yield strength in the through-thickness direction.

In an isotropic material, the tensile and compressive yield strengths are identical, so that yielding under the balanced tension begins when the uniaxial yield strength is reached. For anisotropic materials, however, the uniaxial tensile and through-thickness compressive strength may differ considerably. In (0001) textured sheets of HCP metals, for example, the lack of slip systems suitably oriented to allow thinning may be responsible for high compressive yield strengths in the through-thickness direction and a combined strengthening that may be identified as "texture hardening."

Approach

As discussed in the preceding section, measurement of the R value of the material is a good indication of the degree of texture hardening. Since R is defined as the ratio of the width-to-thickness strains, then a strip type tensile specimen provides a simple and convenient method of determining R. In the example of thin sheets, it is possible to measure the strains in the x and y directions and compute the z strain

using the constancy of volume relationship. However, measurement of the strains in the x, y, and z directions, using plate specimens, will permit a direct determination of the R value. The latter method was used here.

Specimen Selection

Since it is desired to measure an average value of R for the 5Al-2.5Sn ELI titanium alloy, full thickness strip type tensile specimens, as shown in Figure 23, were machined from both the 1/4 and the 1/2 inch thick plates. The four inch wide ends were used to grip the specimens in the testing machine during testing.

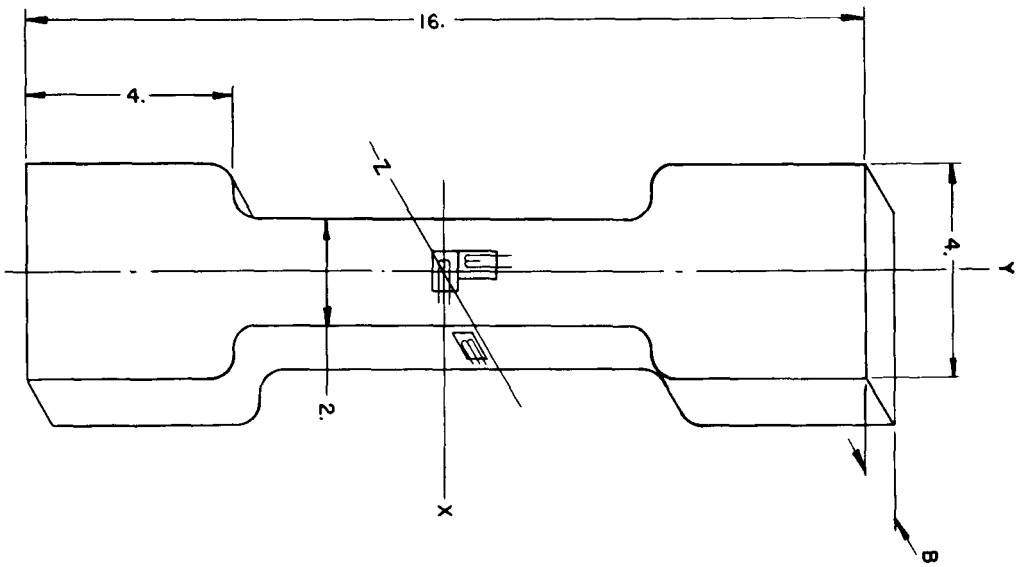

Figure 23. Strip type Tensile Specimen Used to Measure the R Value

Experimental Technique

High elongation metafilm strain gages were applied to the specimen as shown in Figure 23. The specimens were tested in a 300,000-lb tensile machine. Strain gage readings were taken at regular load increments, using a digital read-out strain indicator. Readings were taken up to at least ten percent strain in the y direction.

The texture hardening effect is developed only in the plastic range. In order to conform to the constancy of volume requirements for plastic flow, it is necessary to convert the engineering strains to true strains. The relationship used is

$$\epsilon = \ell n\ (e + 1) \qquad (14)$$

The R values were determined directly by dividing the width strain by the thickness strain.

Experimental Results and Discussion

The R values so determined are plotted as a function of the true strain in the y direction for the 1/4 inch thick 5Al-2.5Sn ELI titanium alloy plate in Figure 24, and for the 1/2 inch thick plate in Figure 25. It will be observed that the R value is relatively low in the elastic range.

At the yield point of the material, the R value is indeterminate. This is presumably due to the gradual change in Poisson's ratio from 0.30 to 0.50 for plastic deformation. However, once the yield point has been exceeded, the R value rises to a maximum value and remains constant with increasing strain. The 1/4 inch thick plate, which had the greater percentage of hot work, showed higher values of R than did the 1/2 inch thick plate. This would be anticipated since the higher percentage of hot work would offer more opportunity for preferred orientation. It will also be noted that the specimen taken transverse to the rolling direction exhibited R values which were higher than those determined using specimens machined parallel to the rolling direction.

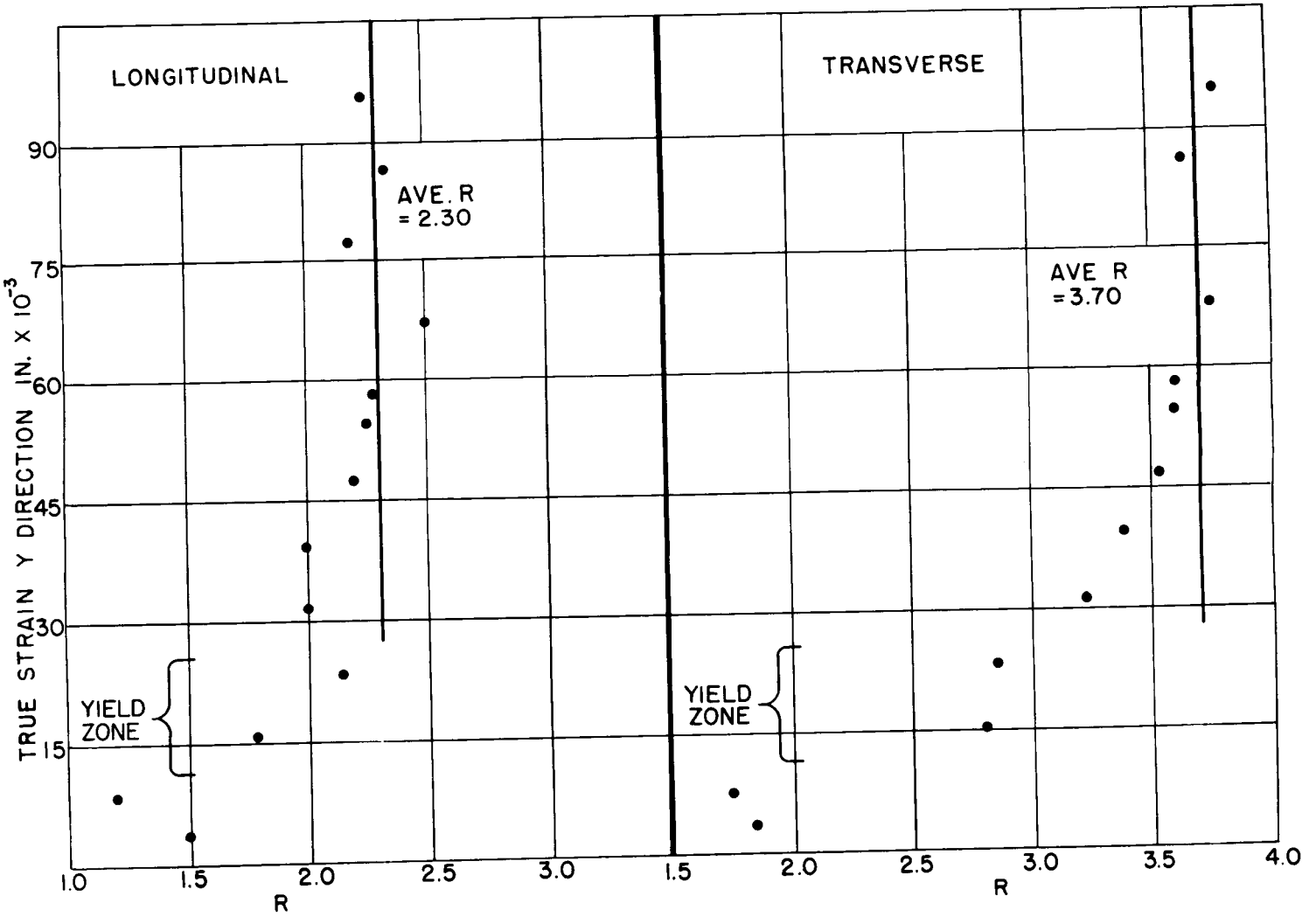

Figure 24. R Value vs True Strain in y direction for 1/4 inch thick 5A1-2.5Sn ELI Titanium Alloy Plate

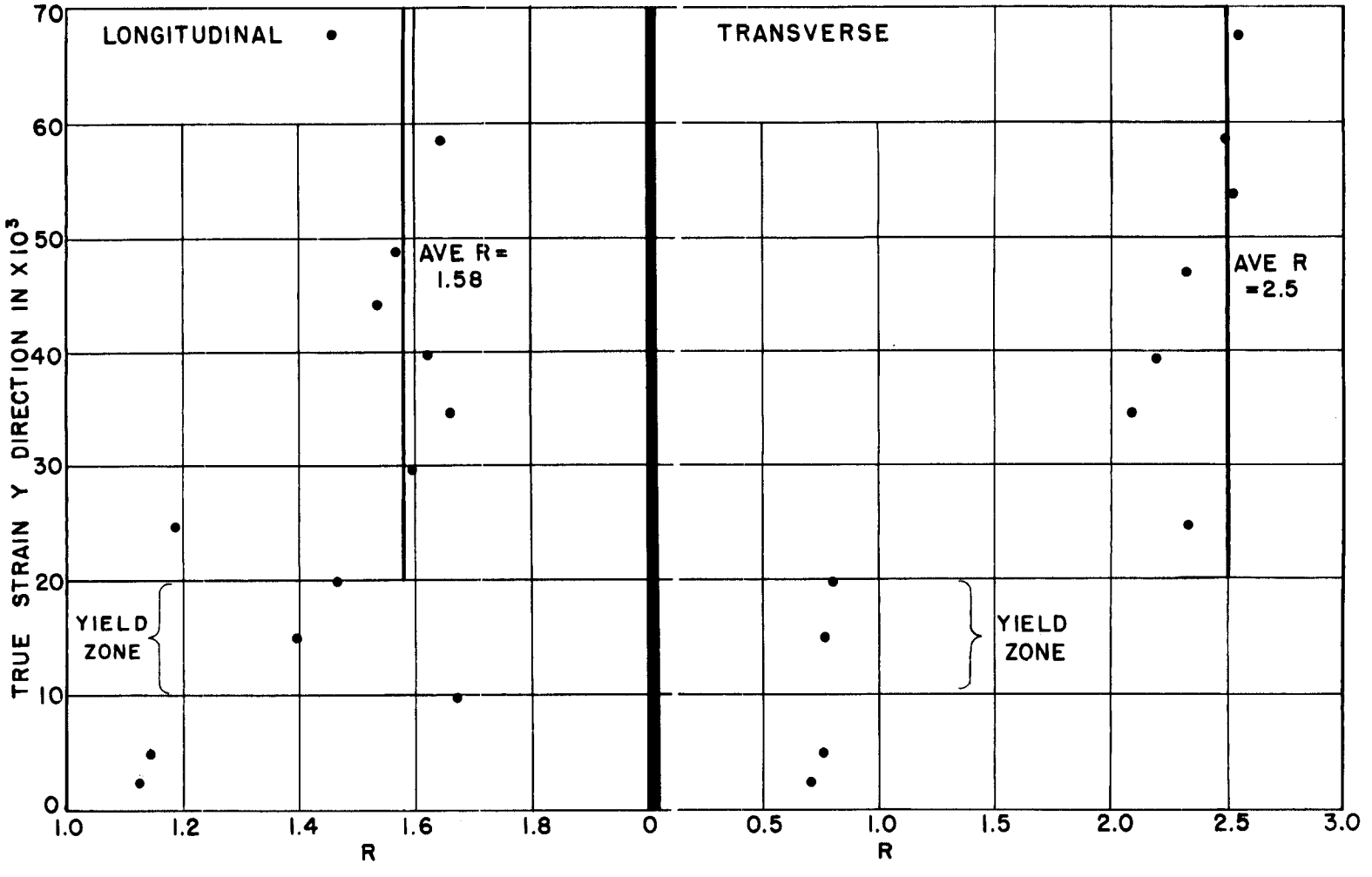

Figure 25. R Value vs True Strain in y direction for 1/2 inch thick 5Al-2.5Sn ELI Titanium Alloy Plate

EFFECT OF PREFERRED ORIENTATION ON
THE PLASTIC FLOW AND FRACTURE OF TITANIUM

Recent work by Hatch[17] has shown that the 5Al-2.5Sn titanium alloy develops a strong (0001) $[10\bar{1}0]$ texture. Pole figures reported by Hatch show that the (0001) pole is normal to the plane of the sheet. For material having a low R value, the pole figure may show a sheet texture with the basal pole split about the normal in the transverse direction. An idealized (0001) $[10\bar{1}0]$ texture is shown in Figure 26.

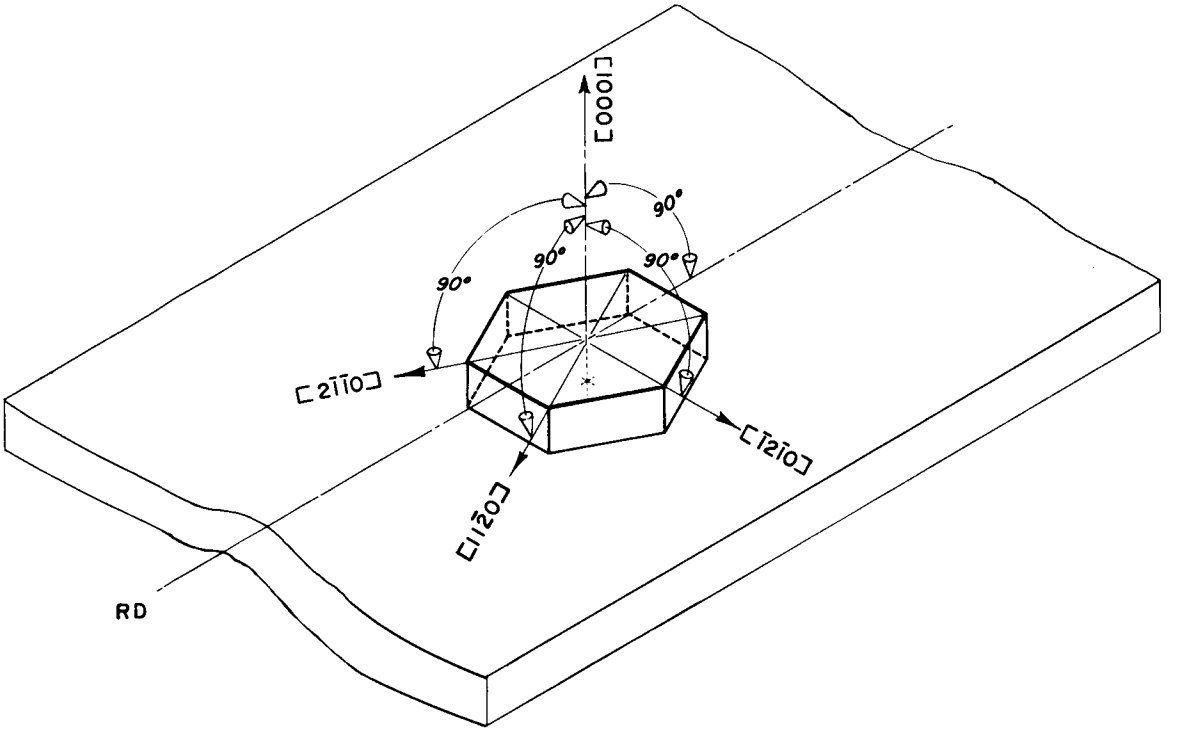

Figure 26. Idealized (0001) $[10\bar{1}0]$ texture

A literature review of the deformation modes in titanium by Holden et al[18] has shown that at least three slip systems are operative at room temperature. These are the $\{10\bar{1}0\}\langle\bar{1}2\bar{1}0\rangle$, $\{10\bar{1}1\}\langle\bar{1}2\bar{1}0\rangle$, and $\{0001\}\langle\bar{1}2\bar{1}0\rangle$. Common to all of these are the slip direction, $\langle\bar{1}2\bar{1}0\rangle$, which lies in the (0001) plane. It is clear that if (0001) is parallel to the sheet plane, deformation by slip through the thickness direction of the sheet would not be possible and a texture-hardened sheet would result. However, three twinning planes at room temperature have also been reported. These are the $\{10\bar{1}2\}$, $\{11\bar{2}1\}$, and $\{11\bar{2}2\}$. The $\{10\bar{1}2\}$ cannot contribute to thinning for an ideal (0001) texture since the c/a ratio of titanium is less than $\sqrt{3}$. On the other hand, an analysis of the crystal geometry for twinning on $\{11\bar{2}1\}$ and $\{11\bar{2}2\}$ will show that both could contribute to thinning from tension in the sheet plane.

Examination of the conditions necessary to form the plastic strain zone ahead of the crack shows that the LD and TD series require plastic flow in the thickness direction of the sheet. In the case of a highly textured material, this is difficult.

In the fracture toughness studies it will be recalled that the K_{Ic} values for the TD series tested at -423° F were higher than those for any other set of experiments. Also, these specimens were oriented in the high R value direction of the plate. Based on the preceding discussion and analysis, the plastic flow would then be initiated by twinning, and the K_{Ic} value should be higher since the twinning stress is usually higher than the shear stress.

A metallographic study was made of the pop-in area of both the LD and TD series of specimens from the 1/2 inch thick 5Al-2.5Sn ELI titanium plate. The results of this examination are shown in Figures 27 and 28. Study of these figures shows a greater area and a higher density of twins in the TD specimen.

The greater tendency toward twinning in the TD series should also be apparent by examination of the fracture surface. Fractographic techniques were used for this phase of the investigation. Replicas were prepared, using the two-stage plastic method. The features observed on the fracture surface of LD series of specimens are shown in Figures 29 and 30. Figure 29 shows the characteristics of the fracture surface associated with twinning, as indicated by the straight line marking. The structure shown in Figure 30 is of the ductile rupture dimple type, indicating that slip, in addition to twinning, is responsible for plastic deformation in this material at -423° F.

The structures observed for the TD series of specimens are shown in Figures 31 and 32. Figure 31 shows the twinning pattern, and Figure 32 illustrates ductile rupture dimples. It will be observed that the twin lines are better developed in this series of specimens than in the LD series. Although it cannot be shown here, the frequency of twinning in the TD series is greater than in the LD series.

Figure 27. Structure Observed along Path of Crack Extension in LD Series Specimen

Figure 28. Structure Observed along Path of Crack Extension in TD Series Specimen

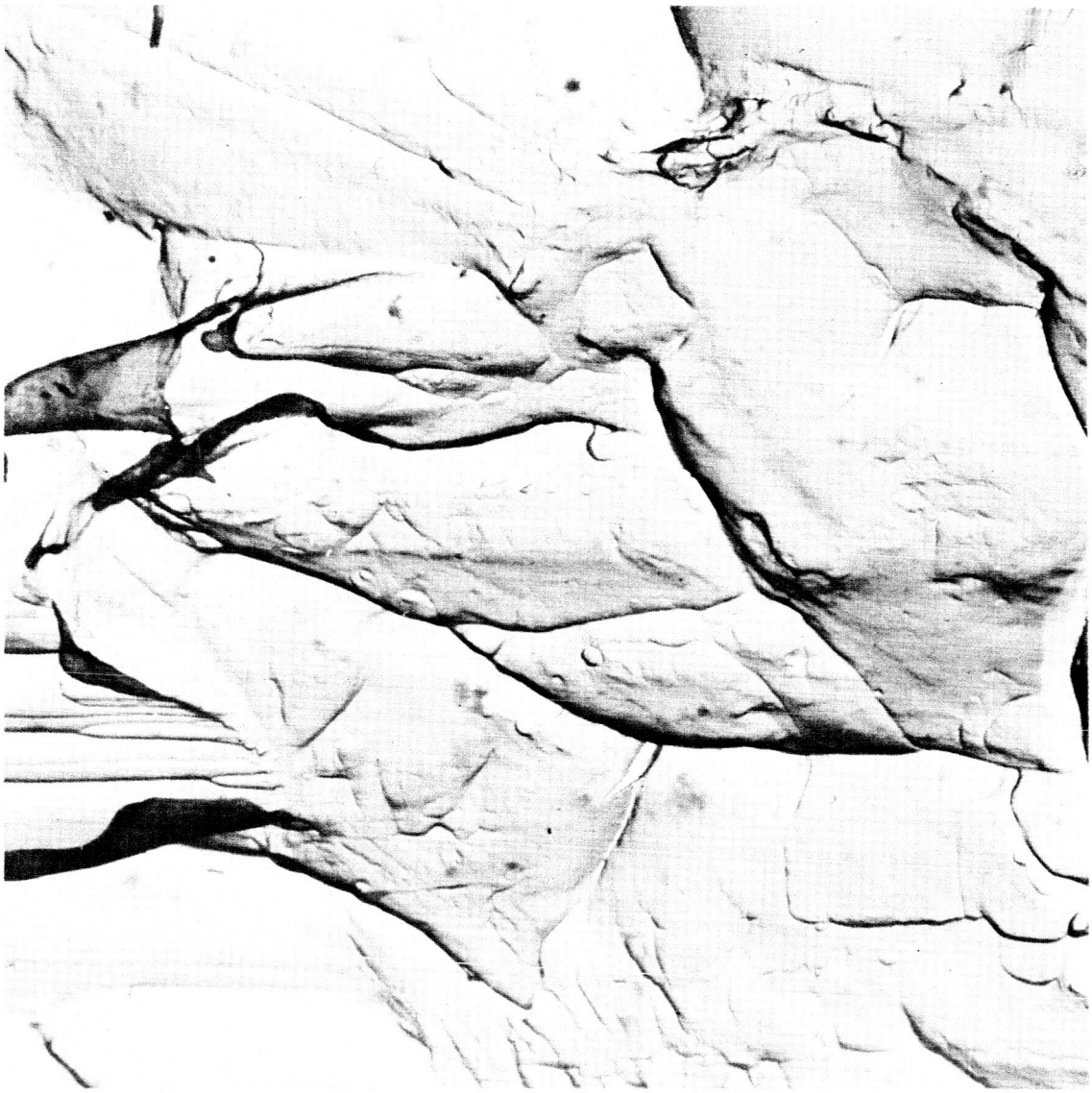

Mag: 7200 X

Figure 29. Fractograph of Specimen LD, showing Twin Formation

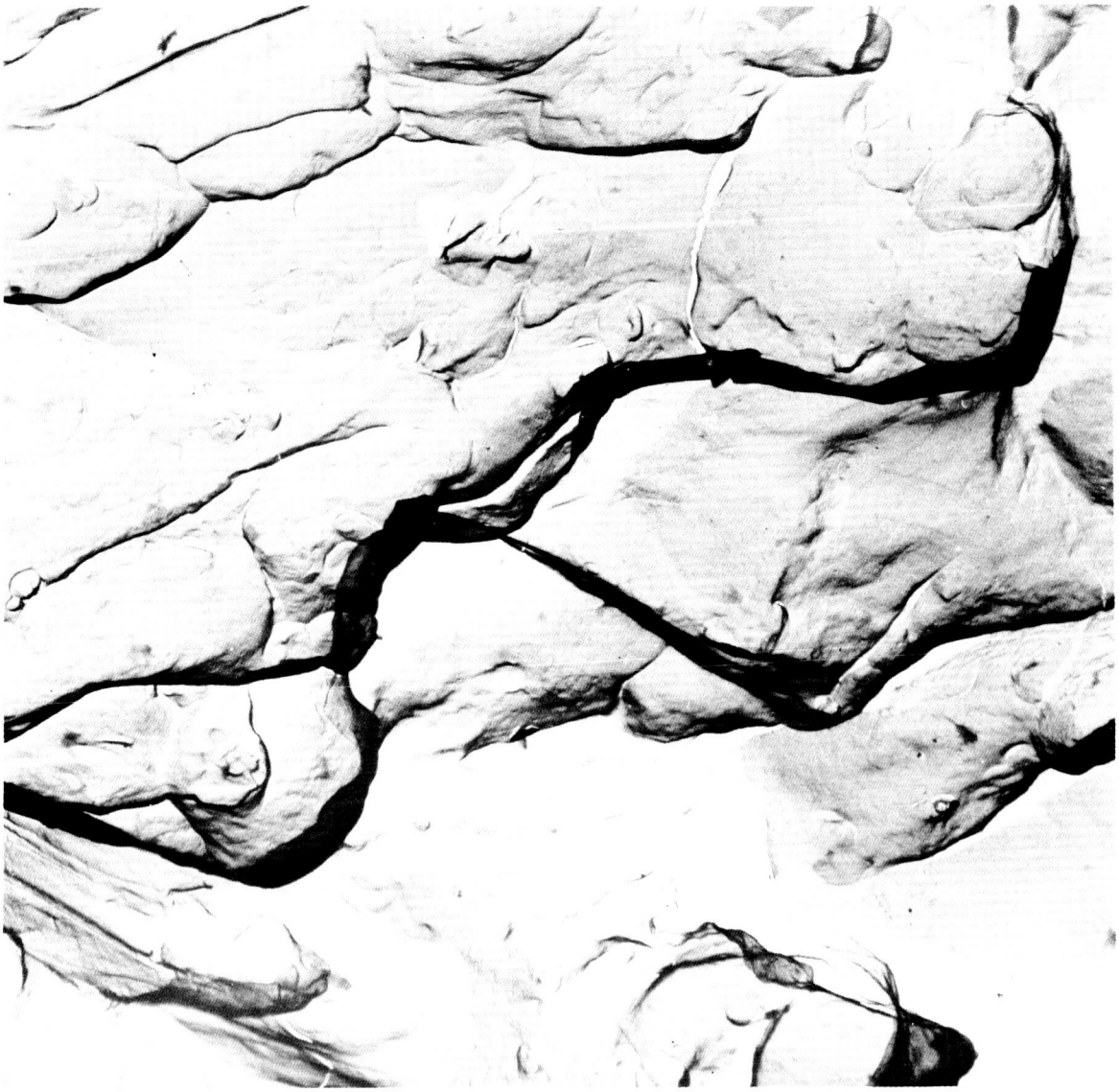

Mag: 7200 X

Figure 30. Fractograph of Specimen LD, showing Ductile Rupture Dimple Formation

Mag: 7200 X

Figure 31. Fractograph of Specimen TD, showing Twin Formation

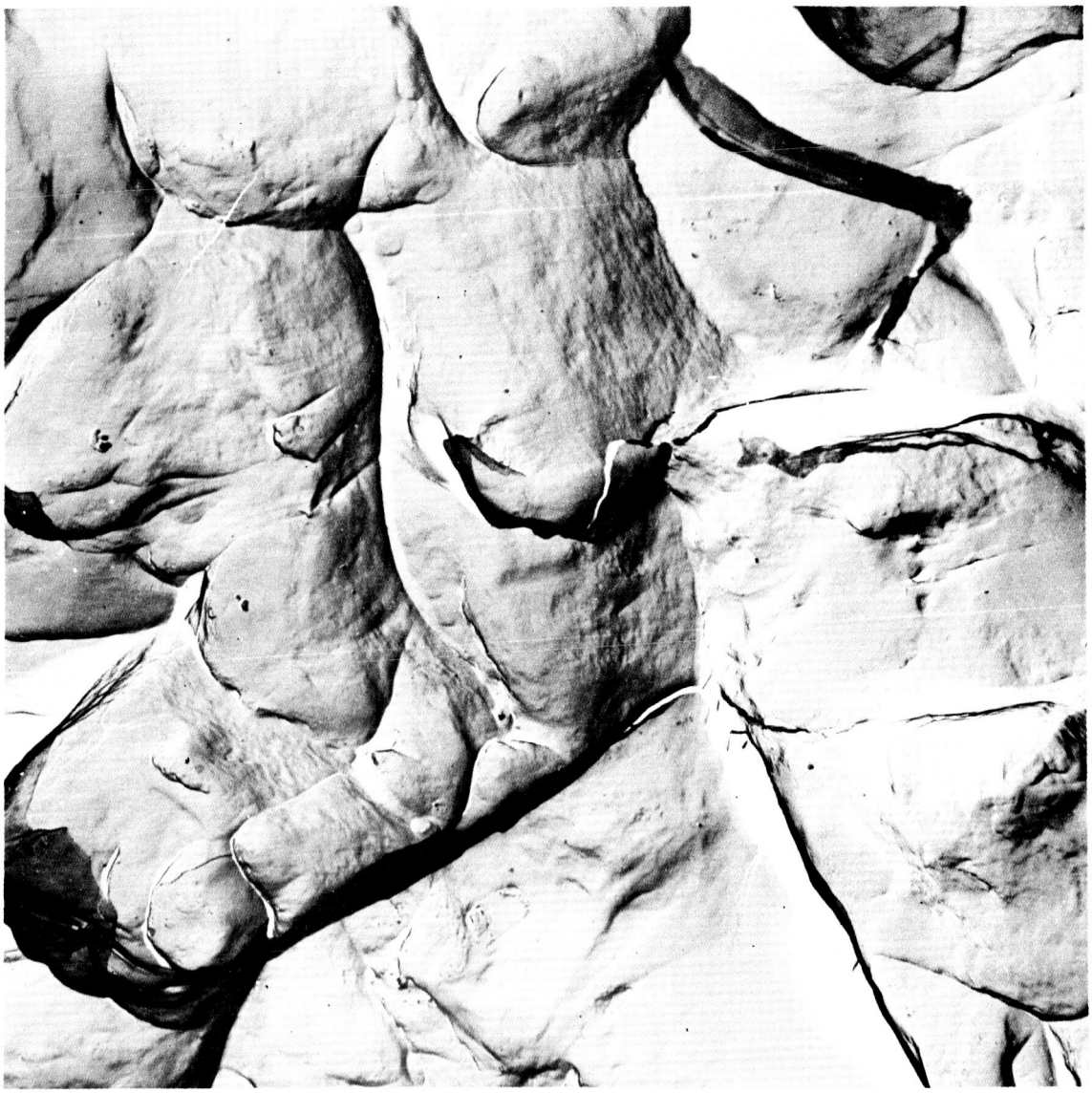

Mag: 7200 X

Figure 32. Fractograph of Specimen TD, showing Ductile Rupture Dimple Formation

DESIGN CONSIDERATIONS

Of the many considerations to which the designer must devote attention, those discussed in this report are: (1) yield stress, (2) plane strain fracture toughness, and (3) texture hardening. These topics will be reviewed in that order.

(1) The data for the yield stress at the various test temperatures have been tabulated and are self-explanatory.

(2) The plane strain fracture toughness may be used to calculate the size and geometry of defects which will become unstable under a given stress. Irwin[5] has defined a parameter, β, as

$$\beta = \frac{K^2}{B\sigma_{ys}^2} \tag{15}$$

and has stated that if $\beta_c = 2\pi$, a through-the-thickness crack of length equal to twice the plate thickness will be stable at the yield stress. The general appearance of the broken single-edge notched specimens from the 1/2 inch plate indicated that, for a first approximation, K_c and K_{Ic} may be taken as equal. Calculation of β_c under these conditions gave a value of 2.88, indicating that a two-plate thickness crack would be unstable.

Calculations of the crack depth for plane strain instability were made using Equation 7. Assuming a semicircular crack geometry and yield stress failure, the crack depth was found to be 0.86 inch. This is greater than the plate thickness. Similar calculations, assuming an infinitely long crack, gave a crack depth of 0.38 inch. Calculation of the radius of the plastic zone at the crack tip gave a value of 0.226. It is evident that the crack and the zone of plasticity extend through the entire plate thickness and, thus, failure will occur at a lower stress than calculated.

Under these conditions, another analysis may be used to calculate the critical size of a through crack using the following equation.

$$K_c^2 = \frac{\pi \sigma^2 a}{1 - \frac{1}{2}\left(\frac{\sigma}{\sigma_{ys}}\right)^2} \tag{16}$$

Solution of this equation for one-half crack length (a), assuming burst stress equal to the yield stress, gave a value of 0.23 inch, or a total crack length of 0.46 inch.

In Figure 33, the crack depth for instability is plotted as a function of gross section stress for a crack which has a surface length four times its depth, using Equation 7. The range of K_{Ic} values shown

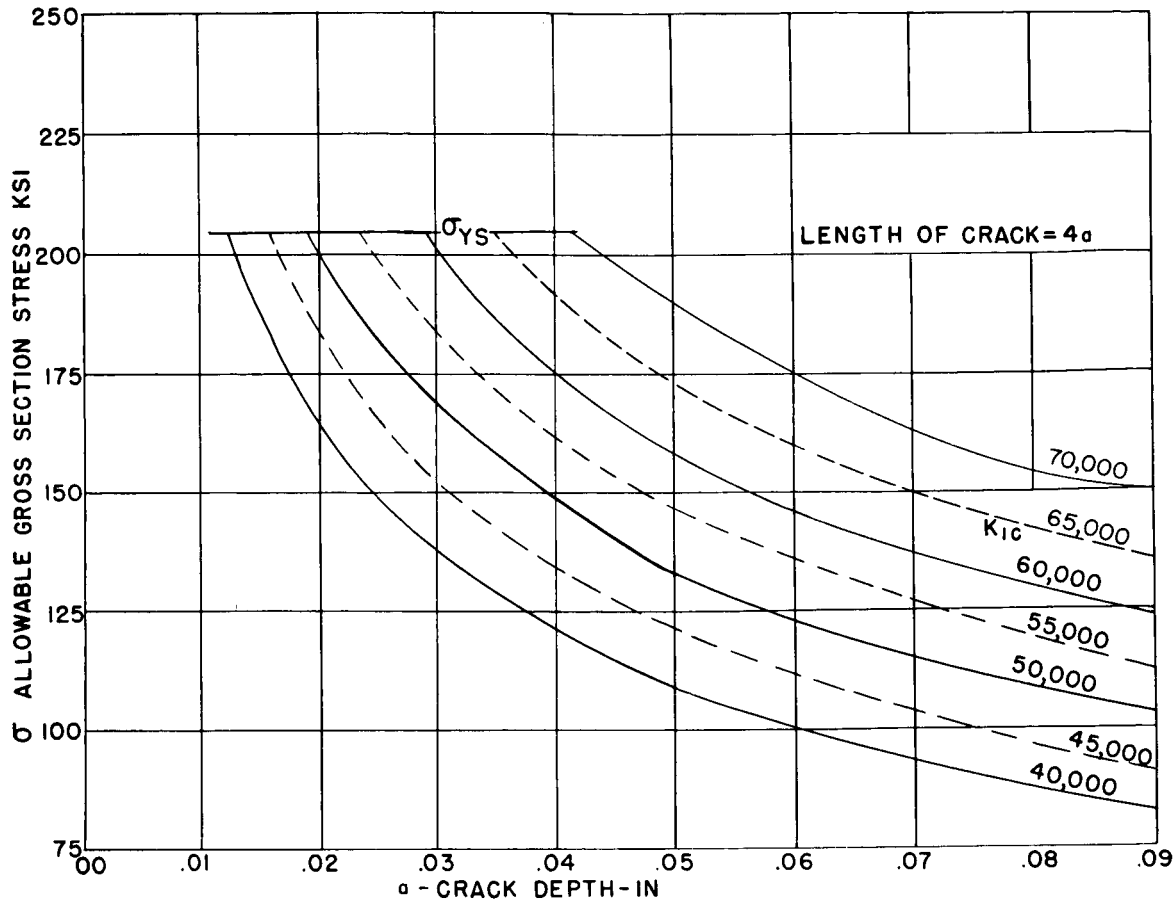

Figure 33. Variation of Critical Crack Depth for Instability as a Function of Applied Stress for Several K_{Ic} Values

here was obtained from this work. This type of plot may be used to establish inspection standards or limit the design stress to account for the minimum size of defect which can be found by nondestructive testing. An example of the use of Figure 33 as an engineering design tool follows.

If a structure were to be fabricated from the 1/2 inch thick 5A1-2.5Sn ELI titanium alloy used in this investigation for service at -320° F, the K_{ic} in the direction of interest would be determined from

Table VII (e.g., LS K_{Ic} = 67,000 psi $\sqrt{in.}$). If the service stress for this structure were approximately 175 kpsi, then the maximum allowable defect depth which could be tolerated (as seen from Figure 33) would be 0.050 inch. If the structure were fabricated from the 1/4 inch material to be used at -423° F and the direction of interest were transverse to the original direction of rolling, the K_{Ic} may be determined as 48,800 psi $\sqrt{in.}$ (from Table IV). If the minimum crack depth which could be detected by nondestructive means were 0.030 inch, the "a" in Figure 33 would be 0.030 inch and the maximum allowable stress at which this structure could be operated would be approximately 167 Kpsi. These values, however, do not include any allowance for a safety factor.

(3) Texture hardening may be used to obtain high burst stresses in many pressure vessel applications. The values of R for the 1/4 and 1/2 inch thick 5Al-2.5Sn ELI titanium alloy plates and the approximate elevation of the burst strength are summarized in Table X. Relatively large increases in the yield stress may be predicted as a consequence of texture hardening. However, care must be taken to avoid brittle fracture

TABLE X
Ratio of Width Strain to Thickness Strain (R)
for 5Al-2.5Sn ELI Titanium Plate

Plate Thickness (in.)	Specimen No.	Direction of y Strain with Respect to Rolling Direction of Plate	Strain Ratio (R)	Avg Value of Strain Ratio	Ratio of Biaxial to Uniaxial Yield*
1/4	4	Longitudinal	2.08		
	6		2.04	2.14	33
	1		2.30		
1/4	5	Transverse	3.70		
	3		3.42	3.40	45
	2		3.08		
1/2	3	Longitudinal	1.58		
	4		1.61	1.60	25
	6		1.61		
1/2	5	Transverse	2.54		
	2		2.50	2.50	37
	1		2.44		

*Using $\sigma = \sqrt{\frac{4(R+1)}{5+R}}\,\sigma_{ys}^2$ and $(\sigma - \sigma_{ys})\ 100$ = percent increase;

where: σ = burst strength, σ_{ys} = yield strength, and R = strain ratio.

CONCLUSIONS

It may be concluded that

1. The tensile properties of 5Al-2.5Sn ELI titanium alloy are sensitive to testing temperature. The tensile yield strength varies from 100,000 psi at room temperature to approximately 200,000 psi at -423° F.

2. The plane strain fracture toughness of this material exhibits an inverse first order dependency on the yield strength. The K_{Ic} values vary from 130,000 psi $\sqrt{in.}$ at a yield strength of 100,000 psi (room temperature) to approximately 55,000 psi $\sqrt{in.}$ at a yield strength of 200,000 psi (-423° F).

3. The 5Al-2.5Sn ELI titanium alloy exhibits essentially an isotropic behavior in regard to plane strain fracture toughness.

4. The plane strain fracture toughness of this material does not appear to be affected by the amount of reduction in the plate. The K_{Ic} values for both the 1/2 inch and 1/4 inch thick plate are essentially the same at the cryogenic temperatures when reliable data could be obtained.

5. The 1/4 inch thick plate exhibits higher R values than the 1/2 inch thick plate and, consequently, a greater potential for elevation of the biaxial yield strength.

REFERENCES

1. C. B. Espy, M. H. Jones, and W. F. Brown, Jr., "Factors Influencing Fracture Toughness of Sheet Alloys for Use in Lightweight Cryogenic Tankage," Symposium on Evaluation of Metallic Materials in Design for Low Temperature Service, Special Technical Publication No. 302, ASTM, 1961.

2. A. A. Griffith, "The Phenomena of Rupture and Flow in Solids," The Philosophical Trans of the Royal Society of London, Vol 221, 1920.

3. G. R. Irwin, "Fracture Dynamics," Fracturing of Metals, pp 147-166, ASM, 1947.

4. C. E. Inglis, "Stresses in a Plate Due to the Presence of Cracks and Sharp Corners," Proceedings of the Institute of Naval Architects, Vol 60, 1913.

5. G. R. Irwin, "Relation of Crack Toughness to Practical Applications," Welding Journal Research Supplement, November 1962.

6. G. R. Irwin, "Crack Extension for a Part-through Crack in a Plate," J of Applied Mechanics, Vol 29; Trans ASME, Vol 84, Series E, 1962.

7. R. W. Boyle, A. M. Sullivan and J. M. Krafft, "Determination of Plane Strain Fracture Toughness with Sharply Notched Sheets," Welding Journal, Vol 41, No. 9, Research Supplement 428-s to 432-s, 1962.

8. B. Gross, J. E. Srawley, and W. F. Brown, Jr., "Stress Intensity Factors for a Single-edge Notched Tension Specimen by Boundary Collocation of a Stress Function," NASA, Lewis Research Center, NASA TN D-2603, January 1965.

9. G. R. Irwin, "The Crack Extension Force for a Crack at a Free Surface Boundary," U.S. Naval Research Laboratory, NRL Report 5120, 15 April 1959.

10. H. F. Bueckner, Internal Reports of the General Electric Co., Schnectady, New York.

11. J. D. Luban, "Experimental Determination of Energy Release Rates for Notch Bending and Notch Tension," Proceedings ASTM, Vol 59, 1959.

12. J. A. Kies, H. L. Smith, H. E. Romine, and H. Bernstein, "Fracture Testing of Weldments," Fracture Toughness Testing and Its Applications, ASTM Special Technical Publication No. 381, 1965.

13. A. Kaufman, "Performance of Electrical Resistance Strain Gages at Cryogenic Temperatures," NASA TN D-1663, March 1963.

14. R. E. Smallman, Modern Physical Metallurgy; Washington, D. C.: Butterworth, Inc.; 1963.

15. J. E. Srawley, "Comparison of Capacities of Various Specimens for K_{Ic} Measurement," Notes for ASTM Committee, May 1963.

16. W. F. Hosford, Jr., and W. A. Backofen, "Strength and Plasticity of Textured Metals," Fundaments of Deformation Processing, Proceedings of Ninth Sagamore Conference; Syracuse University Press, 1964.

17. A. J. Hatch, "Texture Strengthening of Titanium Alloys," Trans AIME, January 1965.

18. F. C. Holden, D. W. Williams, W. R. Riley, and R. I. Jaffe; Battelle Memorial Institute Report TML No. 30, 31 January 1956.

UNCLASSIFIED
Security Classification

DOCUMENT CONTROL DATA - R&D

(Security classification of title, body of abstract and indexing annotation must be entered when the overall report is classified)

1. ORIGINATING ACTIVITY *(Corporate author)*
FRANKFORD ARSENAL, Philadelphia, Pa. 19137
(SMUFA L3300)

2a. REPORT SECURITY CLASSIFICATION
Unclassified

2b. GROUP
NA

3. REPORT TITLE
Plane Strain Fracture Toughness and Mechanical Properties of 5A1-2.5Sn ELI Titanium at Room and Cryogenic Temperatures

4. DESCRIPTIVE NOTES *(Type of report and inclusive dates)*
Technical Research Report

5. AUTHOR(S) *(Last name, first name, initial)*
CARMAN, Carl M.
FORNEY, John W.
KATLIN, Jesse M.

6. REPORT DATE	7a. TOTAL NO. OF PAGES	7b. NO. OF REFS
April 1966	66	18

8a. CONTRACT OR GRANT NO.	9a. ORIGINATOR'S REPORT NUMBER(S)
AMCS 5900.21.11603	R-1796
b. PROJECT NO. NASA Purchase Order C6860A	
c.	9b. OTHER REPORT NO(S) *(Any other numbers that may be assigned this report)*
d.	NASA CR-54296

10. AVAILABILITY/LIMITATION NOTICES
Distribution of this report is unlimited.

11. SUPPLEMENTARY NOTES	12. SPONSORING MILITARY ACTIVITY
	NASA, Lewis Research Center

13. ABSTRACT

The suitability of 5A1-2.5 Sn ELI titanium alloy for cryogenic tankage applications has been studied by determining the mechanical and fracture properties of the material at testing temperatures ranging from room temperature to -423° F. Small round tensile specimens were developed to measure the tensile properties over the range of testing temperatures. Plane strain fracture toughness measurements were also made at these temperatures using the "pop-in" technique with a small notched bend specimen.

Special laboratory techniques were developed to test the specimens at -423° F, utilizing the specific heat of vaporization of liquid helium.

The degree of preferred orientation in this alloy was qualitatively studied by determining the ratio of the width strain to the thickness strain. The fracture toughness values were interpreted in terms of the crystallography and mechanism of deformation of titanium.

The data are summarized in terms of a part-through defect which will be stable at various operating temperatures and stress levels. It has been shown that texture hardening may be used to obtain high burst stresses under biaxial stress conditions.

DD FORM 1 JAN 64 1473

UNCLASSIFIED
Security Classification

14. KEY WORDS	LINK A		LINK B		LINK C	
	ROLE	WT	ROLE	WT	ROLE	WT
Fracture Mechanics Cryogenic Testing Aluminum-Tin-Titanium Alloys Texture Hardening						

INSTRUCTIONS

1. ORIGINATING ACTIVITY: Enter the name and address of the contractor, subcontractor, grantee, Department of Defense activity or other organization *(corporate author)* issuing the report.

2a. REPORT SECURITY CLASSIFICATION: Enter the overall security classification of the report. Indicate whether "Restricted Data" is included. Marking is to be in accordance with appropriate security regulations.

2b. GROUP: Automatic downgrading is specified in DoD Directive 5200.10 and Armed Forces Industrial Manual. Enter the group number. Also, when applicable, show that optional markings have been used for Group 3 and Group 4 as authorized.

3. REPORT TITLE: Enter the complete report title in all capital letters. Titles in all cases should be unclassified. If a meaningful title cannot be selected without classification, show title classification in all capitals in parenthesis immediately following the title.

4. DESCRIPTIVE NOTES: If appropriate, enter the type of report, e.g., interim, progress, summary, annual, or final. Give the inclusive dates when a specific reporting period is covered.

5. AUTHOR(S): Enter the name(s) of author(s) as shown on or in the report. Enter last name, first name, middle initial. If military, show rank and branch of service. The name of the principal author is an absolute minimum requirement.

6. REPORT DATE: Enter the date of the report as day, month, year; or month, year. If more than one date appears on the report, use date of publication.

7a. TOTAL NUMBER OF PAGES: The total page count should follow normal pagination procedures, i.e., enter the number of pages containing information.

7b. NUMBER OF REFERENCES: Enter the total number of references cited in the report.

8a. CONTRACT OR GRANT NUMBER: If appropriate, enter the applicable number of the contract or grant under which the report was written.

8b, 8c, & 8d. PROJECT NUMBER: Enter the appropriate military department identification, such as project number, subproject number, system numbers, task number, etc.

9a. ORIGINATOR'S REPORT NUMBER(S): Enter the official report number by which the document will be identified and controlled by the originating activity. This number must be unique to this report.

9b. OTHER REPORT NUMBER(S): If the report has been assigned any other report numbers *(either by the originator or by the sponsor)*, also enter this number(s).

10. AVAILABILITY/LIMITATION NOTICES: Enter any limitations on further dissemination of the report, other than those imposed by security classification, using standard statements such as:

(1) "Qualified requesters may obtain copies of this report from DDC."

(2) "Foreign announcement and dissemination of this report by DDC is not authorized."

(3) "U. S. Government agencies may obtain copies of this report directly from DDC. Other qualified DDC users shall request through _____."

(4) "U. S. military agencies may obtain copies of this report directly from DDC. Other qualified users shall request through _____."

(5) "All distribution of this report is controlled. Qualified DDC users shall request through _____."

If the report has been furnished to the Office of Technical Services, Department of Commerce, for sale to the public, indicate this fact and enter the price, if known.

11. SUPPLEMENTARY NOTES: Use for additional explanatory notes.

12. SPONSORING MILITARY ACTIVITY: Enter the name of the departmental project office or laboratory sponsoring *(paying for)* the research and development. Include address.

13. ABSTRACT: Enter an abstract giving a brief and factual summary of the document indicative of the report, even though it may also appear elsewhere in the body of the technical report. If additional space is required, a continuation sheet shall be attached.

It is highly desirable that the abstract of classified reports be unclassified. Each paragraph of the abstract shall end with an indication of the military security classification of the information in the paragraph, represented as *(TS)*, *(S)*, *(C)*, *or (U)*.

There is no limitation on the length of the abstract. However, the suggested length is from 150 to 225 words.

14. KEY WORDS: Key words are technically meaningful terms or short phrases that characterize a report and may be used as index entries for cataloging the report. Key words must be selected so that no security classification is required. Identifiers, such as equipment model designation, trade name, military project code name, geographic location, may be used as key words but will be followed by an indication of technical context. The assignment of links, rules, and weights is optional.